



HAL
open science

Clays and carbon nanotubes as hybrid nanofillers in thermoplastic-based nanocomposites – A review

Olawale Monsur Sanusi, Abdelkibir Benelfellah, Nourredine Aït Hocine

► To cite this version:

Olawale Monsur Sanusi, Abdelkibir Benelfellah, Nourredine Aït Hocine. Clays and carbon nanotubes as hybrid nanofillers in thermoplastic-based nanocomposites – A review. *Applied Clay Science*, 2020, 185, pp.105408. 10.1016/j.clay.2019.105408 . hal-03605254

HAL Id: hal-03605254

<https://hal.science/hal-03605254v1>

Submitted on 21 Jul 2022

HAL is a multi-disciplinary open access archive for the deposit and dissemination of scientific research documents, whether they are published or not. The documents may come from teaching and research institutions in France or abroad, or from public or private research centers.

L'archive ouverte pluridisciplinaire **HAL**, est destinée au dépôt et à la diffusion de documents scientifiques de niveau recherche, publiés ou non, émanant des établissements d'enseignement et de recherche français ou étrangers, des laboratoires publics ou privés.



Distributed under a Creative Commons Attribution - NonCommercial 4.0 International License

1 **Clays and carbon nanotubes as hybrid nanofillers in thermoplastic-based**
2 **nanocomposites – A review**

3 **Olawale Monsur Sanusi^{a,*}, Abdelkibir Benelfellah^{a,b}, Nourredine Aït Hocine^{a,*}**

4 ^a *INSA CVL, Univ. Tours, Univ. Orléans, LaMé, 3 rue de la Chocolaterie, BP 3410, 41034*
5 *Blois Cedex, France*

6 ^b *DRII, IPSA, 94200 IVRY-SUR-SEINE, France*

7
8 *Corresponding author.

9 *Email addresses:* olawale.sanusi@insa-cvl.fr (O. M. Sanusi), nourredine.aithocine@insa-
10 cvl.fr (N. Aït Hocine).

11

12

13

14

15

16

17

18

19

20

21

22 A B S T R A C T

23 Components such sensors, aerospace, heat exchanger, armour, storage, automobile and other
24 electronics devices are continuously subjected to fluctuating thermal and mechanical stresses
25 which consequently affect their performance, reliability and lifespan. Aerospace industry, for
26 instance, is also in constant quest for weight reduction to attain fuel efficiency in terms of
27 cost. It is because of these factors that engineering polymers are gaining research prominence
28 in heat management systems, where simultaneous high strength and thermal property with
29 significant low weight are crucial. Meanwhile, montmorillonite and carbon nanotubes are
30 mostly used as reinforcing particles to improve physico-chemical, mechanical and thermal
31 properties of thermoplastic matrices. This review discusses the thermoplastics-based
32 nanocomposites reinforced with the hybrid of montmorillonite and carbon nanotubes, for
33 high-performance applications. Influence of the nanoclay on carbon nanotube dispersion and
34 vice versa were revealed and discussed, while used duo as hybrid in thermoplastic matrices.
35 Consequent interaction of the hybrid nanoparticles within the host matrix influences the bulk
36 properties of nanocomposite: Rheology, morphology, thermal stability, flame retardancy,
37 electrical, mechanical as well as tribology. The hybrid nanofillers synergy favours efficient
38 dispersion without destroying nanoparticles structures, leading to optimized percolation
39 threshold and better properties of the ternary nanocomposites. Prominently, the dependency
40 of bulk properties on nanocomposite morphological characteristics is recognised.

41 *Keywords:* Montmorillonite; thermoplastic; hybrid nanocomposite; synergy; morphology;
42 high-performance

43

44

45 **1. Introduction**

46 As at year 2013, engineering plastics has already recorded a market share of more than
47 19.6 million-metric-ton and forecasted to hit more than 29 million-metric-ton by 2020 (Das et
48 al., 2018). Three decades back, (McCrum et al., 1988) gave two reasons for the unending and
49 the continuous expansion to the use of polymers in Engineering: their robust properties
50 (lightness, toughness, chemical and corrosion resistance); and versatility combined with the
51 speed of shaping operations (Arrigo et al., 2018; Nayak, 2019) at which the raw polymers
52 (and other additives) are transformed to functional hardware products. This is currently
53 witnessed in terms of their applications in aerospace (Kausar et al., 2017; Pitchan et al.,
54 2017), packaging, automobile (Shirvanimoghaddam et al., 2018), defence (Kurahatti et al.,
55 2010; Liu et al., 2016; Venkategowda et al., 2018), anti-corrosion (Kumar et al., 2018),
56 marine, sports, vibration control (Geng et al., 2012), piezoelectric sensor (Hosseini and
57 Yousefi, 2017a) and numerous thermomechanical applications (Shabanian et al., 2016; Yuan
58 et al., 2018).

59 Polymeric nanoparticle-filled composites are currently receiving tremendous attention as
60 they are promising engineering materials with varying properties enhancement courtesy of
61 the various nanoparticles incorporated into the polymer matrix (Mohammed, 2014; Cicco et
62 al., 2017; Klonos and Pissis, 2017; Yuan et al., 2018; Nayak, 2019). The nanoscale particles
63 have exceptional high aspect ratio (surface to volume ratio) that provides the needed
64 engineering features required from polymeric composites (Yue et al., 2014; Klonos and
65 Pissis, 2017). The properties impacted on polymers by these nanofillers focus directly on
66 strengthening mechanical, electrical, optical and thermal behaviours as well as barrier
67 features to temperature and fluids (Marquis et al., 2011; Yuan et al., 2017; Kumar et al.,
68 2018). For few decades back, nanofillers include diatomite, carbon black and pyrogenic silica
69 have been used in polymers as additives without understanding their real influence (Marquis

70 et al., 2011). However, the work of (Usuki et al., 1993) from Toyota Research and
71 Development Group brought limelight and definite roles of nanoclays (typical nanofiller) in
72 polymeric polyamide-6 matrix. Multi-walled carbon nanotubes (CNT), graphene (G),
73 graphene oxide (GO), carbon nanoribbon, nanoclays including halloysite nanotubes (Chiu,
74 2016, 2017a; Raee and Kaffashi, 2018; Ren et al., 2018; Zhu et al., 2018; Aguzzi et al.,
75 2019), make the recent list of commonly used nanofillers (Marquis et al., 2011; Nayak,
76 2019).

77 Therefore, researchers and industries are in constant quest of designing cost-effective,
78 multipurpose and robust nanocomposite system for advanced material applications, especially
79 the primary thermomechanical systems: aerospace, automobile, sensors, conductors,
80 petroleum processing facilities (Kausar et al., 2017). For instance, aircraft industry requires
81 low weight nanocomposites for fuel efficiency without jeopardizing strength, stiffness,
82 thermal conductivity, impact and corrosion resistance as the system is continuously exposed
83 to fluctuating harsh environment (Anbusagar et al., 2018). Moreover, polymer applications in
84 modern thermal and high energy-related fields (electronics, storage and energy transportation,
85 medicines) emphasis great attention to fire safety. This is a subset of heat management that is
86 crucial in improving/securing the service life of a system as well as reduction of hazards by
87 quick transfer of generated heat, which ensures maintenance of practically low temperature
88 on the course of operational service (Chen et al., 2016; Xiao et al., 2016).

89 Nanoclay, a two-dimensional (2D) nanofiller, has been fused into polymer matrices with
90 due mechanical, barrier and fire retardancy properties improvement. Clay platelet structure
91 affords it the formation of protective barrier, once high degree of exfoliation with good
92 dispersion is attained, leading to improved polymer physical performances. At this condition,
93 low loading of clay is required. Clay's high rich intercalation chemistry affords it easy
94 chemical modification and compatibility with polymers. Besides, it can be gotten

95 uncontaminated as mineral with little cost (Santangelo et al., 2011). Similarly, one-
96 dimensional (1D) carbon nanotubes (CNT) continues to impact an exceedingly high electrical
97 (Fang et al., 2019), flame retardancy (Lee et al., 2019), mechanical and thermal properties
98 when incorporated in polymers (Khan et al., 2018; Abidin et al., 2019). The superior aspect
99 ratio, lightweight and thermal conductivity of 2000-6000 Wm⁻¹K⁻¹ (Cao et al., 2019) give
100 CNT its uniqueness.

101 In an attempt towards achieving the polymeric nanocomposite high-performance goal,
102 hybrid/combination of these two dissimilar but distinctive nanofillers is being introduced into
103 polymer matrix to produce ternary nanocomposites. Optimal electrical and thermal
104 conductivities, lowered flammability, high barrier system, corrosion inhibition while
105 improving the mechanical properties are targeted (Kumar et al., 2018; Zhou et al., 2018).
106 Hence, the review provides up-to-date information on high-performance nanocomposites
107 developed strictly with incorporation of hybrid of montmorillonite (nanoclay) and carbon
108 nanotubes in thermoplastic matrices. The influence of the nanoclay on carbon nanotubes and
109 vice versa was discussed. Consequent interaction of the hybrid nanoparticles in
110 nanocomposite was analysed on each of the bulk properties of the nanocomposite such as
111 rheology, morphology, thermal and flame retardancy, electrical and mechanical properties.
112 Finally, a summary of the review and other perspectives were presented.

113 **2. The need for hybrid of nanofillers**

114 Nanofiller roles in the mitigation of the deficiencies of polymers give rise to more novel
115 academia researches and subsequent progressive industrial demands for the composite of
116 thermoplastics, thermosets and elastomers (Marquis et al., 2011; Arrigo et al., 2018;
117 Boumbimba et al., 2018; Aydođan and Usta, 2019). A little percent of nanofillers
118 significantly changes the physicochemical, thermal, mechanical, optical, magnetic and

119 electrical properties of the hosting matrix (Papageorgiou et al., 2017a; López-Barroso et al.,
120 2018).

121 Sizable number of researchers (Bray et al., 2013; Moghri et al., 2015; Kim et al., 2015;
122 Bischoff et al., 2017; Ramazanov et al., 2018; Yuan et al., 2018; Radmanesh et al., 2019)
123 have worked on the benefits of incorporating a single nanoparticle type into selected
124 polymeric matrix (homopolymer, copolymers or mixed polymers), especially in the areas of
125 attaining well dispersed nanofillers for toughening or improving polymeric nanocomposite.
126 However, efficient and effective dispersion without agglomeration of the nanofillers in a
127 polymer remains a challenge (Papageorgiou et al., 2017a; Pitchan et al., 2017; López-Barroso
128 et al., 2018). Another impediment is the incompatibility of the constituent materials
129 (Prashantha et al., 2014).

130 Meanwhile, nanocomposites property enhancement is directly related to the interfacial
131 bonding formation that exists between the reinforcement phase and the matrix
132 (Shirvanimoghaddam et al., 2017). Researchers in their varying efforts of proffering solutions
133 resorted to the use of chemicals (either to modify the filler or as dispersing agent) (Navidfar
134 et al., 2017), which are usually expensive, environmentally demeaning and sometime
135 detrimental to the structure and surface of the nanofiller and/or lowering the properties
136 expected from the bulk nanocomposite (Marquis et al., 2011; Tjong, 2014; Szeluga et al.,
137 2015; Punetha et al., 2017). Other means of realizing an efficient dispersion is through high
138 shear rate, which de-agglomerates the clustered nanofiller particles, and prevents further
139 agglomeration resulted from van der Waals forces of interaction. However, high shear can
140 cause breakage of some CNT or nanofibres particles (Levchenko et al., 2011). Moreover,
141 conductive polymer composite (CPC) is gaining high relevance in the electromagnetic
142 interference (EMI) shielding and carbon-material reinforced CPC is popular in this field. EMI
143 is usually protected by reflection and absorption processes. However, single carbon-

144 reinforced CPC releases secondary EMI pollution because, in this case, the conductivity
145 stems from reflection (Zhao et al., 2018).

146 Hybridization of nanofillers in a matrix provides safe and effective means of ensuring
147 dispersability of certain nanofiller using other nanofiller (Levchenko et al., 2011; Szeluga et
148 al., 2015; Papageorgiou et al., 2017a). Combination of nanofillers could bring about
149 synergistic effects between nanoparticles (Nurul and Mariatti, 2013), offset deficiency in any
150 of the fillers as well as improving and/or aiding dispersion and interaction of the fillers within
151 the polymeric matrix (Safdari and Al-Haik, 2013; Papageorgiou et al., 2017a). Ultimately,
152 benefits of the constituents' fillers are brought together in creating advanced, cost-effective
153 (Pandey et al., 2014; Szeluga et al., 2015) and innovative materials.

154 *2.1. Hybrid fillers in ternary nanocomposites*

155 Hybrid nanocomposite is a system of material that involves the combination of two or
156 more different nanofillers in a single or multiphase polymer matrix with the purpose of
157 achieving better material properties. Hybrid nanocomposite is pivoted on three rules: (1)
158 economic effect by which expensive nanofiller can be combined with less expensive filler;
159 (2) achieving a combined functional and properties enhancement; and (3) efficient
160 preparation method (hybrid effect) (Jaafar, 2017).

161 Researchers used various combinations of fillers in different polymer matrices to achieve
162 properties improvements. Zhao et al. (2018) used both 7 wt% (CNT and Nickel (Ni)) and 13
163 wt% (graphene (G) and Ni) in enhancing heat dissipation for electromagnetic shield. Zhou et
164 al. (2018) recorded over 126% enhancement in thermal conductivity on incorporating 20 wt%
165 of GO and CNT in poly (methyl methacrylate) (PMMA). Edenharter et al. (2016) used a total
166 of 5.5 wt% (GO and layered double hydroxide (LDH)) to realize 47% reduction in peak of
167 heat release rate (PHRR). Xiao et al. (2016) attained 602% in thermal enhancement at hybrid

168 filler load of 22 wt% (G and CNT). With optimum combined nanofillers (ZnO and CNT) of
169 40.5 wt% in poly (butyl methacrylate), Han et al. (2016) reported high thermal stability of the
170 ternary composite with improved tensile strength (42%), elastic modulus (19%) and hardness.
171 Shao et al. (2016) also employed 8.4 wt% (boron nitride (BN) and G) in achieving 350%
172 thermal conductivity improvement. Oliveira et al. (2016) used polyetherimide and CNT
173 doped with sodium alanate (NaAlH₄) for hydrogen storage.

174 Sa et al. (2018) added only 0.8 wt% of CNT and G; and Chatterjee et al. (2012) used 0.5
175 wt% of G and CNT nanofillers to achieve prime mechanical property. Kumar et al. (2010)
176 reported an enhanced thermomechanical properties with just 0.5 wt% of CNT and G. Yang et
177 al. (2011) developed CNT/G/epoxy nanocomposite filled with hybrid of 0.9 wt% G and 0.1 wt%
178 CNT. They reported improvement of 35.4, 27 and 146% in tensile strength, Young modulus and
179 thermal conductivity, respectively. Prasad et al. (2009) used 0.6 wt% total loading CNT and
180 nanodiamond in achieving more than 400% stiffness and hardness boost.

181 From these cited works, carbon-based nanofillers, most especially carbon nanotubes, seem
182 to be consistently used in polymer nanocomposite. CNT is unequal in impacting high
183 mechanical, electrical and thermal properties in polymers (El Rhazi et al., 2018; Li et al.,
184 2018), at comparatively low loading, due to its high aspect ratio leading to its unique capacity
185 in formation of interconnectivity. Yet, combination of nanomaterials at high loading (7-47
186 wt%), which might favour some features (e.g. electromagnetic shielding and flame retarding)
187 (Pan et al., 2014), significantly hamper mechanical properties, processability and hike cost
188 (Alshammari and Wilkinson, 2016; Edenharter et al., 2016).

189 Again, all the excellent features of CNT are worthless in isolation because the high aspect
190 ratio and inter-tubular van der Waals forces keep the CNT nanoparticles together as large
191 clusters (Punetha et al., 2017). Secondly, the solubility of CNT in most organic solvents is
192 exceptionally challenging (Vyas and Chandra, 2018). Szeluga et al. (2015) emphatically

193 stated in their review that the main problem with CNT is cost and quantity of production for
194 industrial applications. This is in agreement with (Roes et al., 2007; Almasri et al., 2018).
195 Other effective carbon-based nanofillers, like graphene and graphene oxide (GO), have
196 similar associated challenges (Punetha et al., 2017). These are some of the reasons that
197 prompted and necessitated the research for hybridizing CNT with other nanofillers.

198 Similar to carbon-based nanofiller, application of small amount of layered clay, like
199 montmorillonite (Mt), gives superior properties impact than larger percent of traditional
200 fillers (e.g. glass fibre, calcium carbonate) (Aït Hocine et al., 2008; Prashantha et al., 2014;
201 Raji et al., 2018) in the enhancement of the hosting matrix (Raji et al., 2016; Rahmaoui et al.,
202 2017). Low loading of clay nanofiller attracts improved barrier performance, easier
203 processability and provide excellent surface appearance (Prashantha et al., 2014). Shabanian
204 et al. (2016) combined Mt and hydrogel in achieving high thermal and mechanical properties
205 simultaneously. Clay has also been effectively used in enhancing tribological property
206 (Golgoon et al., 2015; Azam and Samad, 2018a; Wani et al., 2018). Kausar (2016) used
207 combination of nanogold (Au) and Mt to reinforce polyamide in developing flame retardant
208 composite. There are reports on non-conducting nanoclays aiding CNT's dispersion and
209 assisting in creating volume exclusion (conductive nanoparticles free zone) inside polymeric
210 matrix and consequently led to a reduced percolation threshold (Liu and Grunlan, 2007; Wu
211 et al., 2012; Al-Saleh, 2017; Paszkiewicz et al., 2017). More importantly, apart from being
212 the most reported nanofiller, nanoclay is economically and industrially viable for use as nano-
213 reinforcement in polymeric matrices (Ahamed et al., 2016; Surendran et al., 2018).

214

215

216

217 2.2. Carbon nanotube and nanoclay

218 2.2.1. Structure and properties of carbon nanotubes

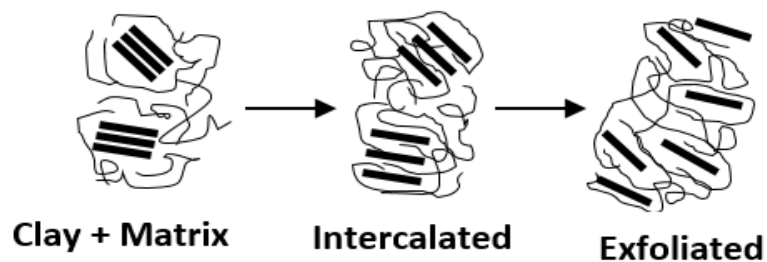
219 Carbon nanotubes (CNT) exhibit unique mechanical, thermal, electric conductivity,
220 electromagnetic interference properties (Zhang et al., 2018) that are impacted onto its hosting
221 polymer matrix. CNT has a ring structure featuring strong bond that is made up of C-C
222 covalent type. This gives CNT its exceptional physical properties but resulted into low
223 affinity to chemical reactions that makes it difficult to interact with other nanofillers as well
224 as polymer matrix molecules (Punetha et al., 2017). Consequently, CNT most often requires
225 surface modifications in enhancing its physicochemical interactions with other molecules and
226 improve its processability (Shirvanimoghaddam et al., 2017). High interfacial relations within
227 polymer nanocomposite brings about effective stress transfer to improve physical, thermal,
228 mechanical, electrical or multifunctional features (Papageorgiou et al., 2017b; Avilés et al.,
229 2018). There are two forms of functionalization, covalent and non-covalent, to get better
230 orientation and improved bonding with matrix (Shirvanimoghaddam et al., 2017, 2018). CNT
231 are available as single, double and multi-walled carbon nanotubes obtained through rolling up
232 of a single or multiple of graphene along its axis. CNT can be produced by arc discharge,
233 laser vaporization, chemical vapour deposition (Manikandan et al., 2013; Safdari and Al-
234 haik, 2018). CNT reported in this review is strictly restricted to multi-walled nanotubes

235 2.2.2. Structure and properties of montmorillonite nanoclay

236 Generally, all nanoclays have the same structural description but are distinguished by their
237 hydroxyl bond relations, positions and interlayer water numbers in each of the clay (Ray and
238 Okamoto, 2003; Raji et al., 2018). They possess two outer tetrahedral ($[\text{SiO}_4]^{4-}$) plates
239 coordinated by silicon atoms and sandwiched on an inner octahedral ($[\text{AlO}_3(\text{OH})_3]^{6-}$) plane,
240 i.e., 2:1 phyllosilicate layered silicate mineral (Barick and Tripathy, 2011). For engineering

241 polymers, montmorillonite (Mt) is crucial and the most reported for polymer nanocomposite
242 preparation because of its unique interfacial reactivity and high specific surface area (Seghar
243 et al., 2011; Bunekar et al., 2018). Mt is a natural phyllosilicate from bentonite and has raw
244 chemical formulae $(\text{Na}, \text{Ca})_{0,3}(\text{Al}, \text{Mg})_2\text{Si}_4\text{O}_{10}(\text{OH})_2, n\text{H}_2\text{O}$ (Marquis et al., 2011).

245 The presence of the compensating charge cations and the polar molecule on the gallery
246 basal planar makes the nanoclay to display the hydrophilic properties, and determines the
247 interlayer space of an expansible clay mineral (Raji et al., 2016). The expansion of the
248 interlayer space with respect to non-expansible clay affords better cation exchange capacity
249 (CEC). Mt has high CEC (Almasri et al., 2018) which is an advantage over other clays. The
250 hydrophilic nature makes clay difficult to be dispersed in polymer and the challenge is
251 addressed through replacement of the interlayer cations by quarternized phosphonium or
252 ammonium cations (Ray and Okamoto, 2003) and sol-gel technique (Bunekar et al., 2018). In
253 short, the interlayer d-value needs to be enlarged in order to allow the penetration of the
254 polymer molecules and/or other nanofiller into clay platelets (Fig. 1).



255
256 **Fig. 1.** Three phases of layered clay in polymer matrix

257 2.2.3. Prepared Mt-CNT hybrid nanofiller

258 Aside physical addition of Mt and CNT into a matrix as regards to this review, the use of
259 Mt-CNT hybrid filler, prepared by growing CNT over Mt via catalytic chemical vapour
260 deposition (CCVD) (Fig. 2) that aids homogenous dispersion within polymer (Manikandan et
261 al., 2013), is also cited. Details on CCVD process can be accessed in (Madaleno et al., 2012).

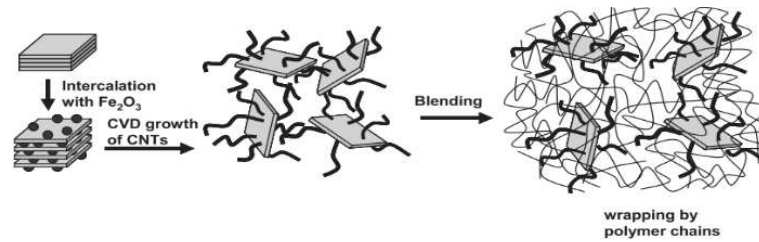


Fig. 2. Route of growing CNT on Mt and blending with polymer (Zhang et al., 2006)

3. Preparation techniques of ternary nanocomposites

Polymer nanocomposite properties are dependent on the processing technique adopted for its production and ultimately dispersion of the nano-reinforcements in terms of effective distribution and exfoliation in the matrix (Zaferani, 2018). Besides the conventional melt blending, solution blending and in-situ polymerization, electrospinning and high-energy ball-milling were recently reported. Table 1 lists the reviewed thermoplastics polymers specifically filled with hybrid of CNT and clay (Mt) for high-performance applications.

Table 1

Summary of thermoplastics polymer filled with hybrid of CNT and Mt.

Matrix	Optimum filler concentration (wt%)			Dispersion Technique	Focused Application	Reference
	CNT	Mt	CNT/Mt**			
ABS	1	1		Melt-mixing	Flame retardant	Ma et al. (2007)
EVA	1	3		Melt-mixing	Thermo-mechanical	Peeterbroeck et al. (2004)
EVA	2.5	2.5		Melt-mixing	Flame retardant cable	Beyer (2005)
EVA	2.5 ^s	2.5 ^s		Melt-mixing	Flame retardant cable	Beyer (2006)
Nafion			2	Solution-mixing	Fuel cell	Manikandan et al. (2012)
HDPE	1	1		Solution- and melt-mixing	Thermo-mechanical	Silva et al. (2014)
HDPE	0.6	0.4		Melt-mixing	Flame retardant	Rao et al. (2015)
UHMWPE	1.5	1.5		Solution-mixing	Tribology	Azam and Samad (2018b)
PA-6			1	Melt-mixing	Mechanical	Zhang et al. (2006)
PCL			0.5	Melt-mixing	Thermo-mechanical	Terzopoulou et al. (2016)
PET			3	Melt-mixing	Thermo-mechanical	Gorrasi et al. (2014)

PLA			3	Centrifugal ball milling	Sorptive and electrical	Santangelo et al. (2011)
PLA			3	Melt-mixing	Irradiation	Gorrasi et al. (2013)
PLA	2	10 [£]		Melt-mixing	Flame retardant	Hapuarachchi and Peijs (2010)
PP	NS	3		Melt-mixing	Mechanical	Olalekan et al. (2010)
PP	0.5*	0.5*		Melt-mixing	Electrical conductor	Levchenko et al. (2011)
PP	1	1		Melt-mixing	Mechanical	Prashantha et al. (2014)
PP	0.3	3		Melt-mixing	Thermal and flame retardant	Pandey et al. (2014)
PP	0.5	0.5		Melt-mixing	Electrical and thermo-mechanical	Al-Saleh (2017)
PS-b-PI-b-PS			1	Solution-mixing	Mechanical	Enotiadis et al. (2013)
PU			0.25	In-situ polymerization	Polymer foam	Madaleno et al. (2013)
PVA			3	Solution-casting	Thermo-mechanical	Zhao et al. (2009)
PVB	0.2	2		Solution-mixing	Impact resistance	Stern et al. (2018)
PVDF	1.9	3		Melt-mixing	Vibration	Geng et al. (2012)
PVDF	0.5	0.5		Melt-mixing	Electrical and thermo-mechanical	Chiu (2014)
PVDF	0.5	1		Melt-mixing	Charge storage	Khajehpour et al. (2014)
PVDF	0.05	0.1		Electrospinning	Piezoelectric	Hosseini and Yousefi (2017b)
PVDF	0.05	0.1		Electrospinning	Sensor Piezoelectric	Hosseini and Yousefi (2017a)

273 *%volume; \$part per resin

274 [£]sepiolite nanoclay; NS not stated

275 **Hybrid CNT/clay produced via CCVD. ABS-acrylonitrile-butadiene-styrene ; EVA-ethylene-vinyl acetate;

276 HDPE-high-density polyethylene; PA-polyamide; PP-polypropylene; PET-poly(ethylene terephthalate); PLA-

277 polylactide; PS-b-PI-b-PS-polystyrene-b-poly(isoprene)-b-polystyrene; PU-polyurethane; PVA-polyvinyl

278 alcohol; PVB-polyvinyl butyral; PVDF-polyvinylidene fluoride; PCL-poly(ϵ -caprolactone); UHMWPE-ultra-

279 high molecular weight polyethylene.

280 3.1. Melt-mixed nanocomposites

281 Melt mixing is a process of applying both high temperature and shear force in order to

282 prepare nanocomposites with well-dispersed nano-reinforcement. It is highly popular for

283 industrial/academic research and development as it supports various forms of polymer that

284 are not suitable for other methods. It requires no solvent/chemical, supports high volume of

285 bulk polymer and it's low cost with the least environmental issues (Bunekar et al., 2018).

286 With regards to the thermoplastics reinforced with hybrid CNT/Mt, many researchers (Zhang

287 et al., 2006; Hapuarachchi and Peijs, 2010; Olalekan et al., 2010; Levchenko et al., 2011;

288 Geng et al., 2012; Chiu, 2014; Khajepour et al., 2014; Pandey et al., 2014; Prashantha et al.,
289 2014; Terzopoulou et al., 2016; Al-Saleh, 2017) have reported properties enhancement with
290 melt-mixing method. Few of the works that draw substantial attention are discussed below.

291 Peeterbroeck et al. (2004) employed melt-blending approach in developing a ternary
292 nanocomposite using CNT and organo-modified Mt in EVA. In the binary system of
293 EVA/Mt, degradation temperature was delayed by 52°C while EVA/CNT composite had only
294 37°C delay. On incorporating hybrid of 3 wt% Mt and 1 wt% CNT nanofillers into the EVA,
295 56°C highest delay was reported. The flammability behaviour was also studied by comparing
296 binary systems (each filled with 4.8 wt% Mt or CNT) and the ternary having the same
297 combined nanofillers loading. All recorded enhanced flame retardancy but ternary
298 EVA/CNT/Mt (CNT:clay; 2.4:2.4) recorded the highest PHRR reduction of 36% with an
299 accompanying lessening of Mt detrimental effect on time to ignition which improved from 67
300 s (Mt/EVA) to 71 s. The ternary supremacy was associated with formation of synergistic
301 uniform crust by Mt/CNT over the burning composite that limited the heat and gas diffusion,
302 and consequently lessened its flammability. Well-dispersed clay platelets, in the presence of
303 CNTs, was reported thus aided the barrier effects.

304 Ma et al. (2007) prepared the hybrid of organoclay and CNT via melt mixing in enhancing
305 ABS flame retardancy. In studying the influence of CNT on clay, morphological state of
306 dispersion of the clay in the composites were analyzed, using X-ray diffraction, in both
307 ABS/2clay (loaded with 2 wt% clay) and ABS/1clay/1CNT (1 wt% clay; 1 wt% CNT). They
308 achieved 3.77 nm interlayer space of the clay in ternary ABS/1clay/1CNT against 3.67 and
309 1.92 nm for binary ABS/2clay and ordinary clay particle respectively. This meant that clay in
310 the ternary attained better exfoliation in the presence of CNT. They also assessed and
311 compared the distribution of filler(s) in both binary and the hybrid-filled ABS. The reported
312 transmission electron microscopy (TEM) affirmed that binary systems prepared with clay,

313 ABS/2Mt, produced composite with insignificant clay exfoliation; and ABS/2CNT with more
314 CNT aggregations within matrix. However, the ternary system revealed CNT intercalated
315 into the Mt interlayer spaces, which produced good interaction between the fillers and matrix
316 structures, and CNT was able to form structured network with the clay platelets. Hence, the
317 superiority of ternary fire retardancy over binary ones.

318 In determining the susceptibility of the residual ash to further heating, they calculated
319 graphitization degree. Ternary ABS/1clay/1CNT reportedly produced ash with higher
320 graphitization than ABS/2CNT, which asserted lower vulnerability of the ternary residual ash
321 to further thermal oxidation on prolonged exposure. They also performed rheological
322 characterizations to further probe into the establishment of 3D network structure by the
323 hybrid fillers, with respect to the single-filled composites. In relation to both storage and loss
324 moduli, the ABS/1clay/1CNT recorded highest values followed by ABS/2CNT and
325 ABS/2clay, while ABS matrix had the least property. They explained the behaviour from
326 nanomaterials' dimensional perspective that the incorporation of high aspect ratio 1D
327 nanotube and 2D nanoclay formed an efficient confined space and created a 3D structure that
328 restricted polymer chains movement. Consequently, enhanced the rheological and flame
329 retardancy characteristics of hybrid-filled nanocomposite over individual nanofiller inclusion.

330 By comparing the processing behaviour of ternary CNT/clay/PP and binary CNT/PP
331 during melt-mixing, Al-Saleh (2017) was able to substantiate reduction in the amount of CNT
332 required for the ternary CNT/clay/PP to attain percolation threshold concentration compared
333 to binary CNT/PP with the same 1 wt% CNT loading. Every two seconds, he monitored the
334 mixing-torque of the nanocomposite against time. It was found that the mixing torque of the
335 binary with only 1 wt% CNT loading was higher than that of ternary system with 1 wt% CNT
336 and 1 wt% clay loading. He concluded that the additional incorporated clay in the ternary

337 served as plasticizers and lowered viscosity, which promoted a reduced shear on the CNT
338 particles. Meanwhile, increase of mixing energy/torque is said to degrade CNT particles.

339 *3.2. Solution-mixed nanocomposites*

340 Solution mixing method gives effective nanofiller dispersion and it involves three main
341 steps: introduction and dispersion of nanofiller(s) into a suitable solvent, mixing with the
342 parent matrix (magnetic, heating, sonication), and drying of the material. Few challenges are
343 inherent with this method: cost and environmental issues linked with chemicals, and the use
344 of ultrasound in aiding polymer solution mixing that may result in reduction of polymer
345 molar mass (Isitman and Kaynak, 2010). Zhao et al. (2009), Manikandan et al. (2012), Azam
346 and Samad (2018b) reported high properties enhancement by adopting this approach in
347 incorporating CNT-Mt hybrid, while Stern et al. (2018) is discoursed for its discovery.

348 Stern et al. (2018) used the hybrid of Mt and CNT to produce PVB-based nanocomposite
349 through solution mixing. In aiding filler(s) dispersion, they applied and varied sonication
350 power (100 W, 700 W), and then studied the effect on morphological and mechanical
351 properties. They reported better dispersions of CNT, clay or hybrid of the fillers in PVB at
352 higher sonication power. Fracture toughness of both hybrid and single-filled matrices
353 affirmed this. At 700 W, ternary PVB/CNT-0.2/nanoclay-2 recorded 176% peak fracture
354 energy improvement while PVB/CNT-0.2 and PVB/nanoclay-2 had 104 and 118%
355 respectively. However, scanning electron microscopy (SEM) and small-angle X-ray
356 scattering (SAXS) employed in studying the nanoclay state of exfoliation revealed a surprise.
357 At 100 W power application, PVB/nanoclay-1wt% and PVB/CNT-0.1wt%/nanoclay-1wt%
358 had interlayer d-values of 17.58 and 17.62 nm; while having 18.36 and 18.34 nm at 700 W
359 sonication respectively, but both were lower than 20.31 nm of the clay particles. This implies
360 a lack of intercalation or exfoliation of the incorporated clays despite the high fracture
361 toughness property of the composites. After that, they found that high surface roughness

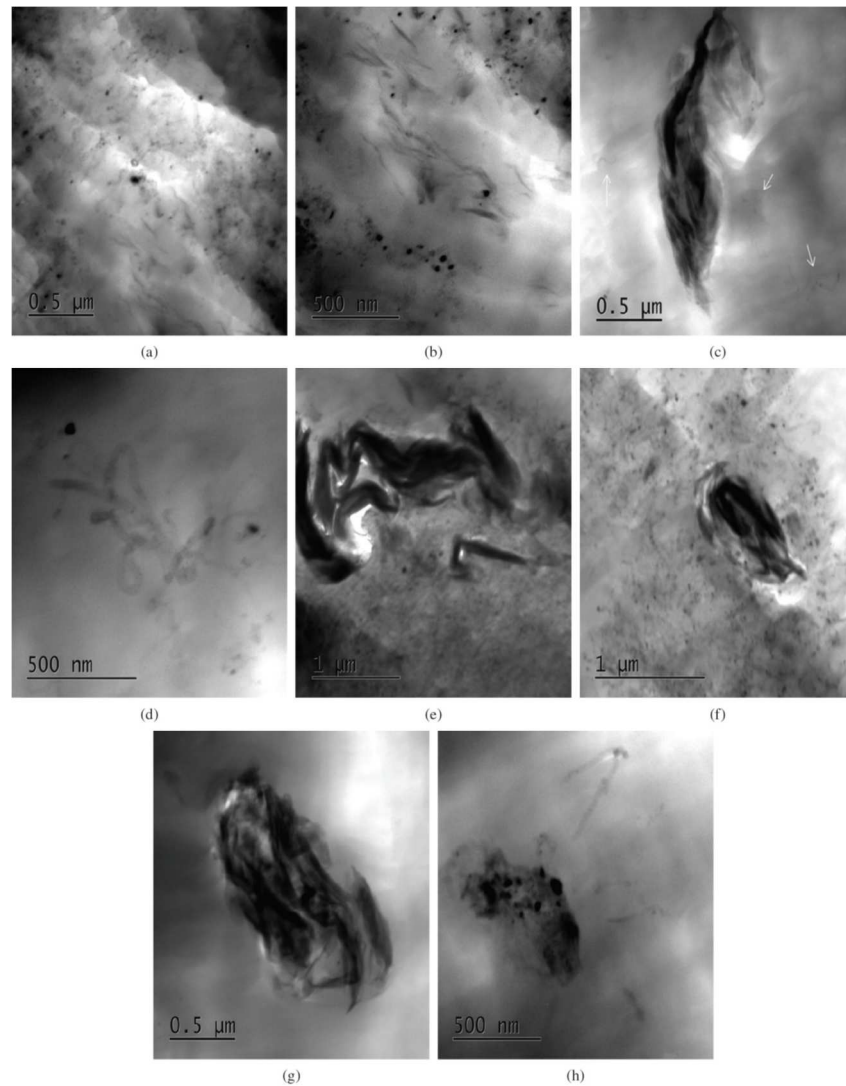
362 value of fractured ternary composite surface, caused by the hybrid fillers synergism, was
363 responsible for the high mechanical property. Consequently, they termed surface roughness
364 as a determinant of fracture toughness aside the famous stress transfer mechanism. Two, high
365 sonication power generates more filler(s) particles which support improved fracture strength.

366 *3.3. Comparing solution-mixing and melt-mixing methods*

367 Silva et al. (2014) compared nanocomposite of HDPE using the hybrid of 1 wt% CNT (C)
368 and 1 wt% of either natural clay (N) or organoclay (30B) by both melt-mixing (m) and
369 solution-mixing (s) methods. The two mixing methods, to prepare binary unmodified natural
370 clay/HDPE, reportedly caused no clay exfoliation in the matrix. Equally, modified clay
371 reportedly remained as agglomerates in HDPE with melt-mixing but well exfoliated with
372 solution method, owing to its organophilic character of swelling to allow HDPE matrix-clay
373 interaction in the presence of solvent. On the contrary, melt-mixing produced better CNT
374 dispersion in HDPE/CNT binary composite than solution method (although inefficient
375 magnetic stirring was reported as the cause of the re-agglomeration of CNT particles). For the
376 ternary nanocomposites by solution blending (Figs. 3a, b, e, f), irrespective of the nanoclay
377 hybridized with CNT, the nanotubes were well dispersed but preferentially formed structure
378 with organoclays (PE/C/30B-s) (Figs. 3a, b). However, ternary composites prepared by melt
379 blending (Figs. 3c, d, g, h) showed agglomerates of nanoclays enclosed by dispersed CNT
380 with some clusters.

381

382



383

384 **Fig. 3.** TEM images at different resolutions for: PE/C/30B-s (a) and (b); PE/C/30B-m (c) and
 385 (d); PE/N/C-s (e) and (f); PE/N/C-m (g) and (h) (Silva et al., 2014)

386 The mechanical study revealed improved Young's modulus irrespective of the preparation
 387 method or clay. Melt-mixed ternary composites got 16% peak enhancement, while binary and
 388 ternary samples with nanoclay via solution mixing only attained 9% modulus improvement.
 389 For hardness, ternary composite (PE/C/30B-s) prepared with organoclay through solution-
 390 mixing recorded 28% peak enhancement but 20% for PE/C/30B-m (melt mixing). They
 391 established the superiority of using organo-modified nanoclay over natural clay as it is more
 392 compatible with CNT in effecting synergistic reinforcement. They explained that the solution

393 mixing offered an easier diffusion of the nanoparticles within the matrix, which contributed
394 to homogenous dispersion of clay/CNT and making them as nucleating agents/sites for
395 crystallization. They also restrained the polymer chains mobility, thus requiring higher load
396 to induce plastic deformation.

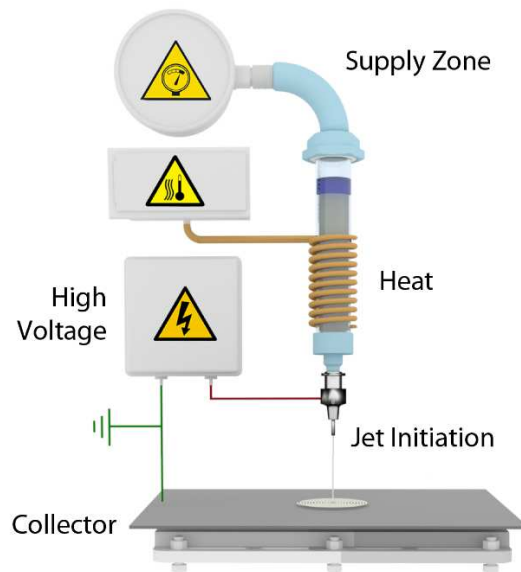
397 *3.4. In-situ polymerization method*

398 Although it was adopted to prepare binary poly(ethylene terephthalate)/clay (Tsai et al.,
399 2014), polyimide/graphene oxide (Wang et al., 2011), nylon-6/graphene (Xu and Gao, 2010),
400 and poly(methyl methacrylate) incorporated with graphene (Potts et al., 2011), in-situ
401 polymerization is rarely compatible with latest techniques of polymer processing (Dlamini et
402 al., 2019) and commonly employed for low viscous matrix like liquid epoxy (Safdari and Al-
403 haik, 2018). To the best of our review, Madaleno et al. (2013) have only applied the method
404 for clay/CNT-filled high-performance thermoplastics polymer nanocomposite.

405 Madaleno et al. (2013) utilized Mt-CNT prepared by CCVD to develop PU nanocomposite
406 foam with varying loading of Mt-CNT (0.25, 0.50, 1.00 wt%). They reported that hybrid
407 fillers at lower concentrations showed no agglomeration, but higher inclusion produced more
408 agglomerates due to the closeness of particles that are of high surface energy and area. All the
409 composites attained improved compressive strength and thermal stability over the neat
410 matrix. Yet, prepared Mt-CNT significantly increased degradation rate of the nanocomposite,
411 associated with metallic particles used in exfoliating clay in CCVD process.

412 *3.5 Electrospinning and high-energy ball milling methods*

413 Electrospinning method can be defined as a process of drawing continuous polymeric fibre
414 from either a polymer solution or polymer melt, based on an electrohydrodynamics
415 phenomenon, using electrostatic force in a liquid-jet form to fabricate polymer composite
416 (Brown et al., 2016). Fig. 4 shows a schematic melt electrospinning system.



417

418

Fig. 4. Melt electrospinning system set up (Brown et al., 2016)

419

420

421

422

423

424

425

426

427

428

429

430

431

432

433

Hosseini and Yousefi (2017a, b) prepared a ternary of PVDF (A), CNT (CN) and modified clay. 0.15 wt% total fillers loading were varied (A/0.05CN/0.1clay, A/0.075CN/0.075clay and A/0.1CN/0.05clay) in studying the effects on PVDF's crystalline structure; and invariably on the piezoelectric performance of the resulting nanocomposites. They observed high level of nanofillers exfoliation in the matrix, for instance, the Mt d-value peak from the XRD disappeared in all composite formulations that connoted a high level of dispersion. They reported reduced composite fibre diameter as the quantity of clay increased (while CNT reduced), that favoured lower viscosity with reduced nanotubes tangles and formation of β -phase crystal, which enhanced the PVDF piezoelectric behaviour. Mt interacted with $-\text{CH}_2$ group in the PVDF, after being stretched by the high electric field during electrospinning, leading to stabilization of targeted β -phase crystals and prevented its transformation to α -phase.

The significant of β -phase content and polarization achieved was verified by piezoelectric impact sensory of neat PVDF, A/0.1CN/0.05clay, A/0.075CN/0.075clay and A/0.05CN/0.1clay composites. They recorded 8.25, 8.4, 9.03 and 10.9 mV/N sensitivities,

434 respectively. They explained that the high sensitivity of A/0.05CN/0.1clay was due to the
435 little amount of the hybrid fillers (0.15 wt%) which was not sufficient to cause any PVDF's
436 polar dilution and detrimental effect on its mechanical flexibility. However, the widest sound
437 absorption by the composite was dependent on higher CNT content (A/0.1CN/0.05clay); and
438 it recorded the least electrical resistance, signifying established network formation at very
439 low loading.

440 Ball milling is another environmental-friendly method adopted by (Santangelo et al.,
441 2011) to developed PLA nanocomposite using clay-CNT nanofiller produced by CCVD
442 growth of CNT over nanoclay (muscovite). Enhanced sorptive and electrical conductivity
443 with 6-9 orders of magnitude in nanocomposite over the pristine matrix was reported. Gorrasi
444 and Sorrentino (2015) wrote a review on forms of mechanical milling for nanocomposite.

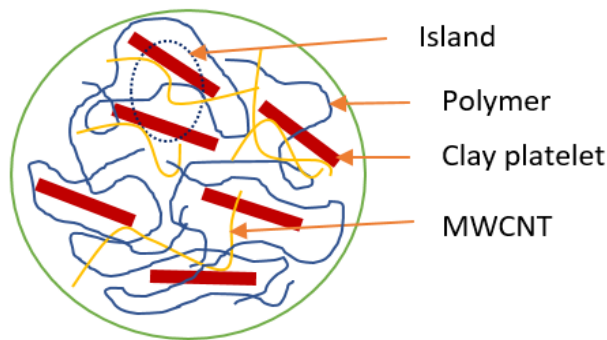
445 **4. Properties of polymeric nanocomposites reinforced with hybrid of nanoclay-CNT**

446 *4.1. Rheological properties*

447 Mixing torque depicts the composite viscosity variations coordinated by the instantaneous
448 microstructural rearrangements. Rheological investigation serves as the tool to evaluate the
449 existing network structure between matrix and the incorporated nanofiller(s) (Rueda et al.,
450 2017; Singla et al., 2017).

451 Pandey et al. (2014) developed ternary nanocomposite comprised of polypropylene (PP),
452 clay (C15A, 3 wt%) and CNT (0.3 wt%) by melt blending. They reported improved storage
453 and loss moduli of all composites over neat PP, while the ternary system had the highest
454 improvement. The same trend was reported for the viscosity of the composites but unlike
455 storage and loss moduli that improved with frequency, viscosity reduced with frequency
456 (non-Newtonian characteristics). The improved rheological behaviour of ternary system over
457 the binary was attributed to the high synergetic interaction of the clay platelets and CNT.

458 CNT has a high degree of affinity for nanoclay, thereby the presence of clay lead to
459 interruption of bundled CNT network and establishing an island of intact clay-CNT three
460 dimensional (3D) network structures that restrain polymer chains motion (see the mechanism
461 in Fig. 5), leading to enhanced viscosity and modulus. The formed intact network effected
462 improved thermal and flammability property of ternary by the formation of protective char
463 with a tight and continuous structure that prevented thermal and mass transfer.



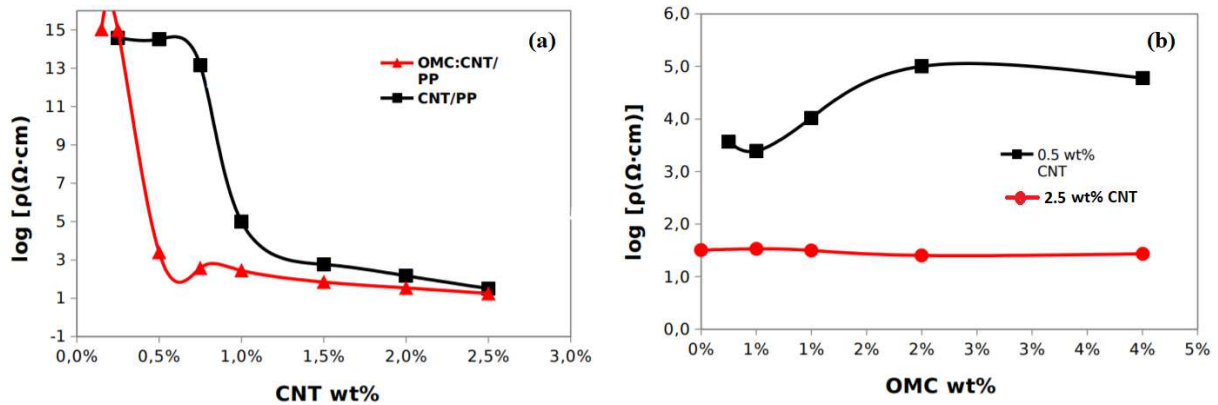
464

465 **Fig. 5.** Clay platelet-CNT interaction mechanism in ternary system

466 Al-Saleh (2017) reported 50% reduction in the quantity of CNT needed for the ternary
467 CNT/clay/PP to attain electrical percolation threshold concentration (EPTC), compared with
468 binary CNT/PP that required 1 wt% CNT (Fig. 6a). The researcher further probed clay
469 influence on electrical resistivity of percolated composites, 0.5 wt% CNT/PP and 2.5 wt%
470 CNT/PP, by adding varying amount of clay. They reported negligible effect on 2.5-CNT/PP
471 because of an established conductive network, while clay increase beyond 0.5-synergistic
472 EPTC upset the "young" CNT-network in 0.5-CNT/PP, with observed resistivity growth (Fig.
473 6b). From rheological study, the researcher found that the mixing torque required by ternary
474 with clay/CNT (having total 2 wt% hybrid fillers) was lesser than the binary composite
475 without clay (only 1 wt% CNT), which was expected to require higher torque. Therefore, the
476 researcher established that the clay inclusion functioned as a plasticizing agent in the matrix
477 that facilitated viscosity and shear stress reduction thereby maintained CNT high aspect ratio,

478 influenced the composite crystallinity and improved CNT-networks formation. This resulted
 479 in a 50% electrical percolation reduction in ternary system. Similarly, Hosseini and Yousefi
 480 (2017b) reported higher dynamic viscosity, storage and loss moduli in electrospun
 481 PVDF/CNT/clay ternary composite compared to neat or single-filled matrix.

482



483

484 **Fig. 6.** (a) Percolation behaviour of CNT/PP with(out) clay (OMC); (b) influence of clay on
 485 electrical resistivity of both 0.5-CNT/PP and 2.5-CNT/PP composites (Al-Saleh, 2017)

486 4.2. Morphological Properties

487 Several examinations are required for better understanding of the structure morphology,
 488 interfacial interaction and nanofillers dispersion in a polymer matrix, like using Raman
 489 microscopy, scanning electron microscopy (SEM), TEM, Fourier transform infrared
 490 spectroscopy (FTIR), X-ray diffraction (XRD). It is worth noting that the morphology of a
 491 nanocomposite dictates its overall performance (Mayeen et al., 2018).

492 Manikandan et al. (2012) utilized CCVD-prepared Mt-CNT fillers to achieve defect-free
 493 homogenous Nafion (perfluoro-sulphnoyl-fluoride copolymer) nanocomposite for fuel cell
 494 application. From microstructural study, strong adhesion in Mt-CNT-Nafion nanocomposite
 495 was proven as broken CNTs particles reportedly remained stuck within matrix. The clay

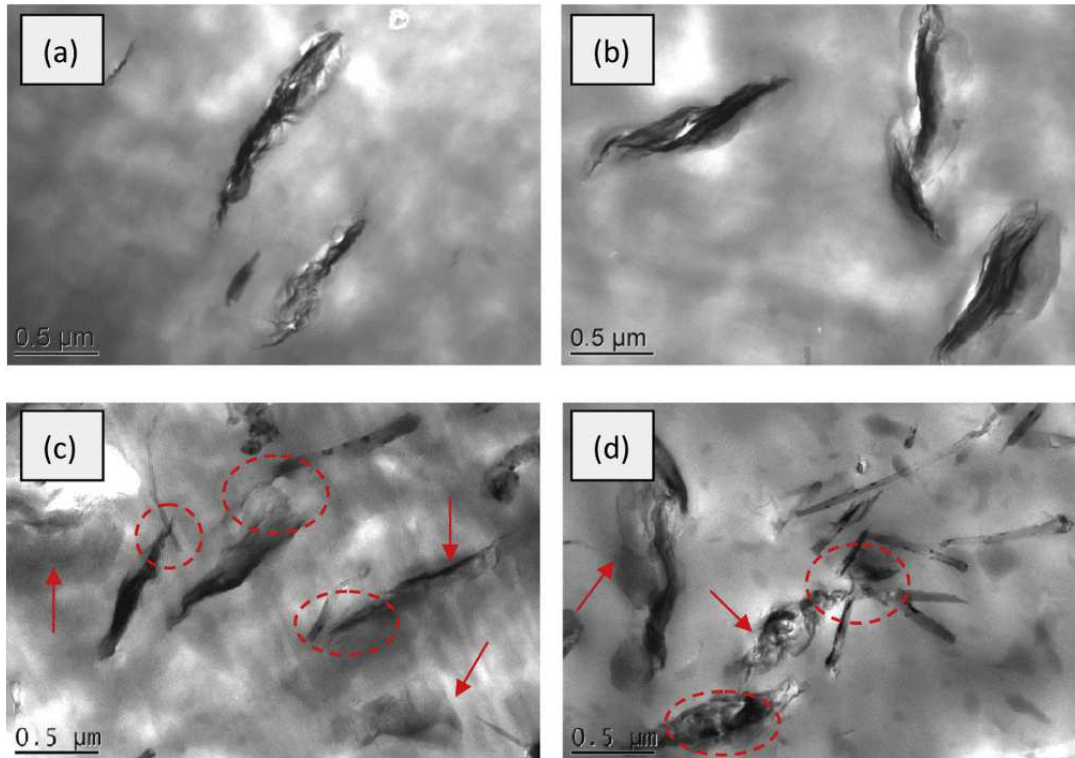
496 layered-structure favoured the uniformity of Nafion over CNT resulted in high thermal
497 stability.

498 Chiu (2014) used the hybrid of Mt (C) and CNT (T) in developing PVDF nanocomposite
499 using melt-mixing approach. Binary and ternary composites of varying nanofiller were
500 prepared with the following designations: C1 (PVDF/Mt-1 wt%), T3 (PVDF/CNT-3 wt%);
501 and CT5 (PVDF/Mt-2.5 wt%/CNT-2.5 wt%). On comparing the morphology of C1 and
502 hybrid reinforced CT5, SEM revealed that the inclusion of CNT aided the dispersion of
503 nanoclay in CT5; unlike Mt aggregation found in C1. Chiu related the behaviour to increase
504 in the melt viscosity when CNT was added to binary PVDF/Mt, which led to intensive
505 dispersion of Mt (Fig. 7). Similarly, on combining CNT with Mt, XRD diffraction angle
506 reportedly shifted to the left and became sharpened, which indicated d-value increase and
507 perfect crystallite size respectively. The morphological study confirmed that the addition of
508 only Mt or the hybrid of the fillers created polymorphism in PVDF matrix. He found that low
509 crystallization cooling rate generated high β -form crystals.

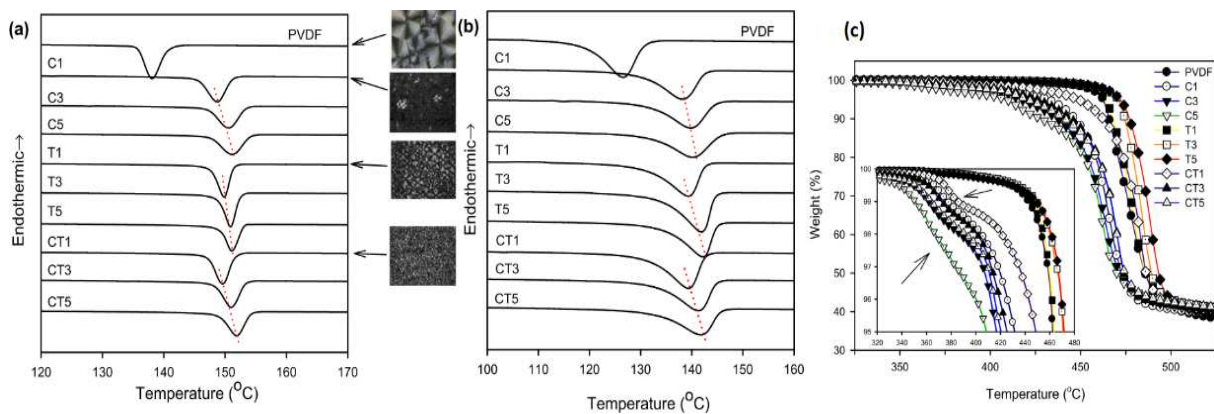
510 He also described the thermal property (DSC) of the composite from the morphological
511 perspectives. It was observed that individual introduction of Mt or CNT and their hybrid
512 (Mt/CNT) significantly acted as nucleating agent for the matrix crystallization which led to
513 increase in both onset and peak crystallization temperatures (Figs. 8 a, b); and these increased
514 with nanofiller mass fraction. Fig. 8a also includes structure of each of the composites and
515 shows the uniformity of structure generated with the use of hybrid filler.

516 In terms of thermal stability, inclusion of CNT in the binary PVDF/CNT (T) improved the
517 thermal degradation of the composite, which suggested good CNT dispersion and protective
518 layer/char formation during heating. However, upsurge of Mt in PVDF matrix led to reduced
519 degradation temperature for the PVDF/Mt (C), while ternary system PVDF/CNT/Mt (CT)
520 displayed thermal stability that falls in between that of the improved binary PVDF/CNT and

521 the reduced binary PVDF/Mt (Fig. 8c). The reduction of thermal stability of Mt-included
 522 composite has been related to the effect of organic modifier on Mt particles. Nonetheless,
 523 CNT upturned the deficiency in Mt while hybridized in the ternary.



524
 525 **Fig. 7.** TEM of PVDF composites containing (a) 1wt% Mt (b) 3 wt% Mt (c) 1.5wt% Mt/1.5
 526 wt% CNT (d) 2.5wt% Mt/2.5wt% CNT (Chiu, 2014)



527
 528 **Fig. 8.** (a) DSC cooling curve $15^{\circ}\text{C min}^{-1}$; (b) $40^{\circ}\text{C min}^{-1}$ (c) TGA curves- N_2 of PVDF and
 529 its composites (Chiu, 2014)

530 *4.3. Thermal and flame retardancy properties*

531 Polymer combustion cycle involves thermal decomposition that yields volatile as well as
532 highly inflammable organic compounds, at comparatively low temperature, and emits large
533 quantum of heat that causes further polymer degradation and accelerates growth of fire
534 (Rothon and Hornsby, 1996; Dasari et al., 2013). Several approaches are used for protection
535 against fire by interrupting the combustion cycle: modification of thermal degradation
536 process, oxygen denial, or inhibition of back-flow of heat (Rothon and Hornsby, 1996; Dasari
537 et al., 2013). Flame retardants (Dasari et al., 2013) or intumescent flame retardants (Yuan et
538 al., 2017) are added to polymer to improve flame retardancy. However, environmental and
539 health-related concerns, aside high loading that has a deteriorating impact on processability
540 (Rothon and Hornsby, 1996; Bourbigot et al., 2019) and mechanical behaviour of resulting
541 nanocomposite (Feng et al., 2018), pose a major challenge.

542 Nanomaterials present eco-friendly flame, smoke and toxicity performances at a very low
543 loading percentage due to its high aspect ratio (Yuan et al., 2017). Few examples include
544 layered silicates (Liu et al., 2019; Zhu et al., 2019), carbon nanotubes (Ji et al., 2018),
545 graphene oxide (Fanga et al., 2019; Wang et al., 2019). Beyer (2005, 2006) attained about
546 57% reduction of PHRR on incorporation of 2.5 phr each of CNT and nanoclay in poly
547 (ethylene-vinyl acetate) copolymer. The heat release capacity was drastically reduced by 58%
548 on incorporation of 2 wt% CNT and 10 wt% clay in PLA matrix (Hapuarachchi and Peijs,
549 2010). Rao et al. (2015) prepared flame retardant nanocomposite of HDPE with blend of
550 modified clay and CNT. They reported improved thermal stability in the binary system with
551 CNT (1 wt%) over the neat HDPE; while with incorporation of only clay (1 wt%) thermal
552 stability fell below pristine HDPE. HDPE/clay binary composite recorded 123.2 and
553 132.16°C for its onset and peak degradation temperatures respectively, while 127.5 and
554 135.34°C for HDPE/CNT in the same order. Meanwhile, simultaneous addition of same ratio

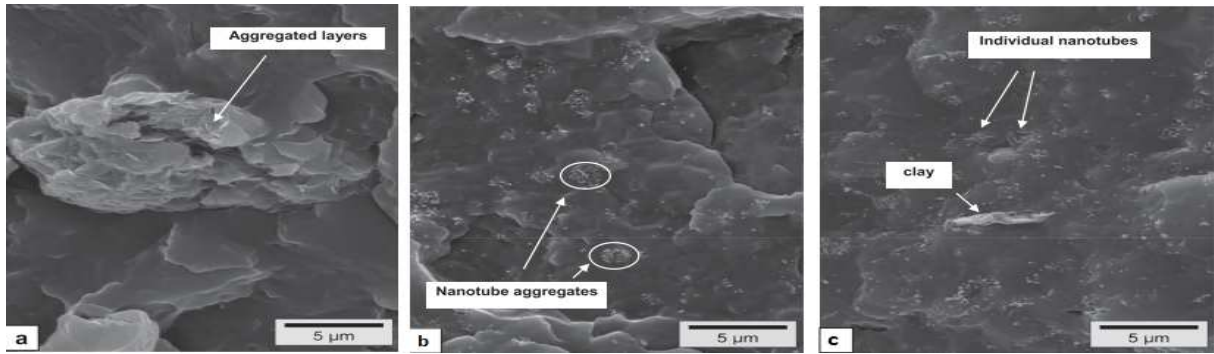
555 of CNT (0.5 wt%) and clay (0.5 wt%) in the matrix showed the best thermal properties: 12%
556 char residue, highest delay in degradation temperatures (onset, 128.1°C; peak, 137.94°C) and
557 the least percentage crystallization that means efficient components interaction.

558 Also, in an effort to determine the optimum ratio of CNT to clay (total loading: 1 wt%) for
559 flammability resistance application in the ternary HDPE/CNT/clay, nanoclay was varied in
560 0.8 - 1 wt% (i.e., CNT 0.2 - 0 wt%) and vice versa. In comparison with neat HDPE, they
561 reported 66.8% reduction in peak heat release rate (PHRR) at optimum formulation of
562 0.6CNT/0.4clay/HDPE. They reported that CNT migrated faster than clay to the matrix
563 surface in forming insulating protective layer, which prevented gas or energy transport. Time
564 to ignition was said to be favoured with CNT increase, as formed char layers served as heat
565 sinks that deferred ignition and degradation. Ternary's mechanical property was also
566 enhanced through enhanced interfacial adhesion, clay exfoliation and CNT dispersion.

567 *4.4. Electrical Property*

568 Levchenko et al. (2011) adopted both experimental and theoretical approach in
569 determining the influence of clay (OC) inclusion on electrical percolation threshold of ternary
570 PP/CNT/OC nanocomposite. Electrical percolation threshold was reported to reduce by
571 28.4% (from 0.95 to 0.68 vol% of CNT) on incorporation of clay into PP/CNT. The
572 behaviour was ascribed to clay disentangling and prevention of CNT aggregations during
573 melt-mix processing, thereby interparticle-contact numbers were enriched to form conductive
574 network. They corroborated this explanation by morphological study that showed clusters of
575 clay or CNT in the singly filled PP/OC or PP/CNT composites, respectively (Figs. 9a, b).
576 Conversely, the SEM image of the ternary showed well-exfoliated CNT at the instance of
577 clay with an established network structure needed for conductivity (Fig. 9c).

578 On the contrary, Khajehpour et al. (2014) reported an increase of percolation threshold on
579 addition of clay to CNT/PVDF from 0.3 to 0.5 wt% of CNT due to deterioration of the
580 conductive network caused by the clay platelets barrier role.



581
582 **Fig. 9.** SEM image of (a) PP/OC (b) PP/CNT (c) PP/CNT/OC (Levchenko et al., 2011)

583 4.5. Mechanical Properties

584 Zhang et al. (2006) incorporated CNT-clay nanofiller, prepared by CCVD process, into
585 polyamide-6 (PA6) by melt mixing. Tensile modulus and strength were enhanced
586 significantly by 289% and 153% respectively. Homogenous dispersion of CNT-Mt was
587 reported and attributed to swollen and exfoliation of clay by iron ions intercalation into clay
588 interlayers as well as CNT growth on clay platelets resulted in enhanced mechanical property
589 of the ternary prepared with 1 wt% of CNT-clay. Olalekan et al. (2010) utilized masterbatch
590 of polypropylene-clay (PP/clay) and CNT in preparing ternary composite. They reported
591 PP/clay composite with tensile strength, Young's modulus and impact strength of 28.55 MPa,
592 1588.27 MPa and 5.55 kJ m⁻², respectively. With incorporation of CNT alongside Mt, they
593 achieved improved tensile strength, Young's modulus and impact strength by 27, 42 and 13%
594 respectively. It was related to higher aspect ratio and specific surface area of the incorporated
595 CNT, and clay facilitated CNT superior dispersion in the matrix and in turn enhanced the
596 mechanical properties of the ternary composite. Geng et al. (2012) reinforced PVDF with
597 CNT and Mt. The mechanical properties of the ternary reportedly surpassed the neat PVDF

598 and single-filled nanocomposites. The reported dynamic mechanical analysis (DMA) showed
599 that the ternary PVDF/1.9CNT/3Mt had approximately twice mechanical loss factor ($\tan \delta$)
600 than binary composites, with an established conductive network and piezoelectric phase,
601 which made the ternary to be applicable for damping application.

602 Prashantha et al. (2014) developed polypropylene (P) nanocomposite reinforced with
603 hybrid (1:1) of Mt (C) and CNT (M). Both binary (MP-2, MP-4, CP-2, CP-4) and ternary
604 (MCP-2, MCP-4) composites showed increase in strength and modulus with nanofillers
605 loadings. Meanwhile, composites with the hybrid fillers recorded better improvements in
606 tensile strength (MCP-2, 37%; MCP-4, 54%) and tensile modulus (MCP-2, 40%; MCP-4,
607 50%). Also, ternary MCP-2 (CNT 1 wt%; Mt 1 wt%) was reported to have the least
608 elongation reduction when compared with neat PP due to increased polymer chains rigidity as
609 a result of nanofillers restriction effects. For hybrid-filled composites, positive synergy in
610 both flexural strength (MCP-2, 49%; MCP-4, 64%) and modulus (MCP-2, 58%; MCP-4,
611 65%) were also reported. The notched ternary composites MCP-2 and MCP-4 maintained
612 respective peak impact strength improvement of 50% and 53% above the neat matrix. The
613 high mechanical properties of the ternary nanocomposites were related to strong clay-CNT
614 and fillers-matrix interfacial adhesions revealed by morphology study. Uniform distribution
615 of retained broken CNT upon failure, instead of pull-out from the matrix, was cited as the
616 factor for property improvement.

617 Terzopoulou et al. (2016) studied the mechanical behaviour of poly(ϵ -caprolactone)
618 incorporated with clay-decorated CNT filler. The hybrid nanofiller was varied: PCL/clay-
619 CNT 0.5 wt%, PCL/clay-CNT 1.0 wt% and PCL/clay-CNT 2.5 wt%. They reported increase
620 in yield point and Young's modulus (stiffness) with the increase in fillers loading, which was
621 related to composite enhanced crystallinity. However, only PCL/clay-CNT 0.5 wt% recorded
622 increase in elongation with respect to the neat matrix. Also, PCL/clay-CNT 0.5 wt% and

623 PCL/clay-CNT 1.0 wt% had respective 5.5 and 3.7% increase in tensile strength but
624 PCL/clay-CNT 2.5 wt% showed 15.9% reduction. Apparently, 0.5 wt% clay-CNT enhanced
625 the composite strength, but higher loading led to weak fillers/PCL interfacial bonding
626 because of agglomeration.

627 *4.6. Tribology Property*

628 Polymeric nanocomposites are fast replacing the traditional materials in fabricating
629 mechanical elements (clutches, bush, gear, and bearing) and other electromechanical systems
630 that solely depend on friction, wear and lubrication principles (Wani et al., 2018). Achieving
631 high tribology efficiency requires homogenous distribution of fillers within matrix.

632 Azam and Samad (2018b) employed solution mixing in preparing UHMWPE
633 nanocomposite using hybrid of Mt (C15A) and CNT for marine application. The samples
634 were designated as Sample, Sample-1, Sample-2, Sample-3, Sample-4, Sample-5, and
635 Sample-6 representing respectively 1.5wt%C15A/UHMWPE, 0.5wt%CNT/UHMWPE,
636 1.5wt%CNT/UHMWPE, 3wt%CNT/UHMWPE, 0.5wt%CNT/1.5wt%C15A/UHMWPE,
637 1.5wt%CNT/1.5wt%C15A/UHMWPE, and 3wt%CNT/1.5wt%C15A/UHMWPE. Cyclic
638 sliding wear test was performed at 9 N load, underwater. Neat UHMWPE failed as early as
639 22000 cycles, while none of the binary and ternary composites failed at the condition. By
640 increasing force to 12 N on composites, they found that only Sample-2 (1.5 wt% CNT) and
641 Sample-5 (1.5 wt% CNT/1.5 wt% C15A) sustained wear life up to 150000 cycles. The earlier
642 failure of neat matrix and other samples was either attributed to lack of CNT, inadequate
643 CNT causing inept matrix chains anchoring, aggregation of CNT or formation of dual-phase
644 structures. These caused weak filler(s)-matrix bonding and poor bridging of the polymer
645 chains resulting in an inefficient loading transfer by the CNTs on the course of wear tests.
646 Interestingly, SEM study of Sample-2 and Sample-5 was reported to reveal homogenous
647 filler(s) dispersion that promoted matrix-filler interactions, polymer chains bridging, and thus

648 secured against any pull out during wear test. On further investigation of the two samples,
 649 ternary Sample-5 displayed its superiority up to 300000 cycles, which indicated the
 650 significant role of the hybrid nanoclay/CNT fillers over single-filled Sample-2 that failed at
 651 170000 cycles.

652 For Sample-5 (with hybrid nanofillers), clay was said to create a torturous path, due to its
 653 platelet structure, which prevented water molecule absorption (transportation) while the CNT
 654 synergistically bridged the polymer chains together during wear test underwater. As hardness
 655 is a critical factor for high wear property, report of 17.14, 12.4 and 2.7% influence of water
 656 on the hardness of neat polymer, Sample-2 and Sample-5 respectively confirmed the synergy
 657 in ternary.

658 **5. Polymer blend reinforced with Mt-CNT Nanofillers**

659 Although this review focusses on a thermoplastic matrix reinforced with Mt-CNT
 660 nanofillers, it is worth considering that researchers have also incorporated the hybrid fillers
 661 into polymer blends (Table 2) and reported magnificent properties enhancement.
 662 Incorporation of Mt/CNT in blend reportedly led to co-continuous morphology formation
 663 (Potschke et al., 2007; Al-Saleh, 2015), mechanical (Chiu, 2017b) and flammability
 664 (Ambuken et al., 2014) properties augmentation.

665 **Table 2**

666 Summary of thermoplastics blends filled with hybrid of CNT and Mt.

Matrix		Optimum hybrid filler concentration (wt%)		Dispersion technique	Focused application	References
I	II	CNT	Mt			
PE	PP	1*	1*	Melt-mixing	Electrical & mechanical	Al-Saleh (2015)
PC	PP	2	3	Melt-mixing	Electrical	Pötschke et al. (2007)
PC	PVDF	2	1	Melt-mixing	Thermo-mechanical	Chiu (2017b)
PU	PA-11	3.5	3.5	Melt-mixing	Thermo-mechanical	Ambuken et al. (2014)

667 *%volume

668 **6. Conclusion**

669 This review has provided the advances on high-performance thermoplastics ternary
670 nanocomposites specifically prepared by the sole incorporation of montmorillonite clays and
671 carbon nanotubes. Preparation of nanocomposites through the conventional and the recent
672 approaches was briefly summarized. Systematically, the reviewed studied each of the bulk
673 properties of nanocomposite: rheology, morphology, thermal, mechanical, electrical, and
674 tribology. Factors responsible for these properties enhancement were identified, and overall
675 nanocomposite behaviour was found to be principally hinge on the resulting morphology.

676 The hybrid fillers influence high properties, though how efficient the influence is solely
677 depended on their level of dispersion within the matrix because agglomeration of any or both
678 of the nanofillers substantially reduce or cause more detrimental effect on the resulting
679 nanocomposite. There is no gainsaying in the significant of rheological property of the
680 composite emanating from right material selection, formulation and other processing
681 variables.

682 The review established the effectiveness of clay in aiding the dispersion of CNT by
683 lowering the viscosity of polymer thereby reducing the CNT percolation threshold, which
684 significantly affects material cost. Clay interjects bundled CNT particles as CNT has a high
685 degree of affinity for nanoclay. Consequently, aiding the formation of network structures that
686 favour electrical and thermal conductivity, and restrict polymer chains movement thereby
687 enhances flame retardancy and mechanical behaviour. Similarly, the presence of CNT
688 facilitates clay d-value increase that leads to improved exfoliation of clay.

689 However, there is need for more research pertaining to the implications of processing
690 behaviour on the ternary nanocomposites. Processing factors, such as temperature, shear and
691 time residence that ultimately affect the resulting nanocomposite properties, should be further
692 studied while using Mt and CNT as hybrid filler in polymers.

693 The superior reduction of the peak of heat release rate (PHRR) is mostly reported in the
694 ternary system, which is related to the formation of synergistic uniform crust by Mt-CNT
695 over the burning composite. Thus limits the heat and gas diffusion and consequently lessen
696 the nanocomposite flammability. Nanoclay modification processing/chemicals should be
697 carefully selected as it is majorly cited to be responsible for early degradation of ternary
698 nanocomposite.

699 For tribology application, clay creates a tortuous path (due to its platelet structure) that
700 prevents molecule absorption (transportation) by nanocomposite while CNT synergistically
701 bridged the polymer chains together resulting in improved wear resistance. Another key role
702 of clay is the creation of polymorph phase in polymer, and CNT inclusion is responsible for
703 the establishment of co-continuous morphological formation in polymer blend.

704 Thermal conductivity is vital in the design of material for heat management services: it
705 improves and guarantees the service life of a system as well as the reduction of hazards.
706 Concurrently, mechanical durability cannot be traded-off in advanced applications such as
707 aerospace, automobile, military and other thermomechanical facilities.

708 **Declarations of interest:** none

709 **Acknowledgements**

710 This work was supported by the Petroleum Technology Development Fund – Nigeria
711 [Grant Number: 18GFC/PHD/065].

712

713

714

715 **References**

- 716 Abidin, M.S.Z., Herceg, T., Greenhalgh, E.S., Shaffer, M., Bismarck, A., 2019. Enhanced
717 fracture toughness of hierarchical carbon nanotube reinforced carbon fibre epoxy
718 composites with engineered matrix microstructure. *Compos. Sci. Technol.* 170, 85–92.
719 <https://doi.org/10.1016/j.compscitech.2018.11.017>
- 720 Aguzzi, C., Donnadio, A., Quaglia, G., Latterini, L., Viseras, C., Ambrogi, V., 2019.
721 Halloysite-Doped Zinc Oxide for Enhanced Sunscreening Performance. *ACS Appl.*
722 *Nano Mater.* xxx, xxx–xxx. <https://doi.org/10.1021/acsanm.9b01482>
- 723 Ahamed, F., Phang, S.W., Sin, T.L., 2016. Mechanical behaviour of thermoplastic
724 starch/montmorillonite/alumina trihydrate nanocomposites. *J. Eng. Sci. Technol.* 11,
725 1344–1359.
- 726 Aït Hocine, N., Médéric, P., Aubry, T., 2008. Mechanical properties of polyamide-12 layered
727 silicate nanocomposites and their relations with structure. *Polym. Test.* 27, 330–339.
728 <https://doi.org/10.1016/j.polymertesting.2007.12.002>
- 729 Al-Saleh, M.H., 2017. Clay/carbon nanotube hybrid mixture to reduce the electrical
730 percolation threshold of polymer nanocomposites. *Compos. Sci. Technol.* 149, 34–40.
731 <https://doi.org/10.1016/j.compscitech.2017.06.009>
- 732 Al-Saleh, M.H., 2015. Effect of Clay Addition on the Properties of Carbon Nanotubes-Filled
733 Immiscible Polyethylene/Polypropylene Blends. *J. Macromol. Sci. Part B Phys.* 54,
734 1259–1266. <https://doi.org/10.1080/00222348.2015.1085753>
- 735 Almasri, D.A., Rhadfi, T., Atieh, M.A., McKay, G., Ahzi, S., 2018. High performance
736 hydroxyiron modified montmorillonite nanoclay adsorbent for arsenite removal. *Chem.*
737 *Eng. J.* 335, 1–12. <https://doi.org/10.1016/j.cej.2017.10.031>
- 738 Alshammari, B.A., Wilkinson, A., 2016. Impact of carbon nanotubes addition on electrical,
739 thermal, morphological, and tensile properties of poly (ethylene terephthalate). *Appl.*

740 Petrochemical Res. 6, 257–267. <https://doi.org/10.1007/s13203-016-0161-2>

741 Ambuken, P. V., Stretz, H.A., Koo, J.H., Messman, J.M., Wong, D., 2014. Effect of addition
742 of montmorillonite and carbon nanotubes on a thermoplastic polyurethane: High
743 temperature thermomechanical properties. *Polym. Degrad. Stab.* 102, 160–169.
744 <https://doi.org/10.1016/j.polymdegradstab.2014.01.017>

745 Anbusagar, N.R.R., Palanikumar, K., Ponshanmugakumar, A., 2018. Preparation and
746 properties of nanopolymer advanced composites: A review, in: Jawaid, M., Khan, M.M.
747 (Eds.), *Polymer-Based Nanocomposites for Energy and Environmental Applications*.
748 Woodhead Publishing Series in Composites Science and Engineering, pp. 27–73.
749 <https://doi.org/10.1016/B978-0-08-102262-7.00002-7>

750 Arrigo, R., Ronchetti, S., Montanaro, L., Malucelli, G., 2018. Effects of the nanofiller size
751 and aspect ratio on the thermal and rheological behaviour of PEG nanocomposites
752 containing boehmites or hydrotalcites. *J. Therm. Anal. Calorim.* 134, 1667–1680.
753 <https://doi.org/10.1007/s10973-018-7555-6>

754 Avilés, F., Cauich-Rodríguez, J. V., Toro-Estay, P., Yazdani-Pedram, M., Aguilar-Bolados,
755 H., 2018. Improving carbon nanotube/polymer interactions in nanocomposites, in:
756 Rafiee, R. (Ed.), *Carbon Nanotube-Reinforced Polymers From Nanoscale to*
757 *Macroscale*. Elsevier, pp. 83–115. <https://doi.org/10.1016/B978-0-323-48221-9.00005-4>

758 Aydoğan, B., Usta, N., 2019. Fire behaviour assessment of rigid polyurethane foams
759 containing nanoclay and intumescent flame retardant based on cone calorimeter tests. *J.*
760 *Chem. Technol. Metall.* 54, 55–63.
761 https://doi.org/https://dl.uctm.edu/journal/node/j2019-1/7_17_223_p_55_63.pdf

762 Azam, M.U., Samad, M.A., 2018a. A novel organoclay reinforced UHMWPE nanocomposite
763 coating for tribological applications. *Prog. Org. Coatings* 118, 97–107.
764 <https://doi.org/10.1016/j.porgcoat.2018.01.028>

765 Azam, M.U., Samad, M.A., 2018b. UHMWPE hybrid nanocomposite coating reinforced with
766 nanoclay and carbon nanotubes for tribological applications under water with/without
767 abrasives. *Tribol. Int.* 124, 145–155. <https://doi.org/10.1016/j.triboint.2018.04.003>

768 Barick, A.K., Tripathy, D.K., 2011. Effect of organically modified layered silicate nanoclay
769 on the dynamic viscoelastic properties of thermoplastic polyurethane nanocomposites.
770 *Appl. Clay Sci.* 52, 312–321. <https://doi.org/10.1016/j.clay.2011.03.010>

771 Beyer, G., 2006. Flame retardancy of nanocomposites based on organoclays and carbon
772 nanotubes with aluminum trihydrate. *Polym. Adv. Technol.* 17, 218–225.
773 <https://doi.org/10.1002/pat.696>

774 Beyer, G., 2005. Filler blend of carbon nanotubes and organoclays with improved char as a
775 new flame retardant system for polymers and cable applications. *Fire Mater.* 29, 61–69.
776 <https://doi.org/10.1002/fam.866>

777 Bischoff, E., Goncalves, G.P.O., Simon, D.A., Schrekker, H.S., Lavorgna, M., Ambrosio, L.,
778 Liberman, S.A., Mauler, R.S., 2017. Unrevealing the effect of different dispersion
779 agents on the properties of ethylene-propylene copolymer/halloysite nanocomposites.
780 *Mater. Des.* 131, 232–241.
781 <https://doi.org/https://dx.doi.org/10.1016/j.matdes.2017.06.033>

782 Boumbimba, R.M., Coulibaly, M., Peng, Y., N'souglo, E.K., Wang, K., Gerard, P., 2018.
783 Investigation of the impact response of PMMA-based nano-rubbers under various
784 temperatures. *J. Polym. Res.* 25, 76. <https://doi.org/10.1007/s10965-018-1479-5>

785 Bourbigot, S., Sarazin, J., Samyn, F., Jimenez, M., 2019. Intumescent ethylene-vinyl acetate
786 copolymer: Reaction to fire and mechanistic aspects. *Polym. Degrad. Stab.* 161, 235–
787 244. <https://doi.org/10.1016/j.polymdegradstab.2019.01.029>

788 Bray, D.J., Dittanet, P., Guild, F.J., Kinloch, A.J., Masania, K., Pearson, R.A., Taylor, A.C.,
789 2013. The modelling of the toughening of epoxy polymers via silica nanoparticles: The

790 effects of volume fraction and particle size. *Polymer (Guildf)*. 54, 7022–7032.
791 <https://doi.org/10.1016/j.polymer.2013.10.034>

792 Brown, T.D., Dalton, P.D., Hutmacher, D.W., 2016. Melt electrospinning today: An
793 opportune time for an emerging polymer process. *Prog. Polym. Sci.* 56, 116–166.
794 <https://doi.org/10.1016/j.progpolymsci.2016.01.001>

795 Bunekar, N., Tsai, T., Huang, J., Chen, S., 2018. Investigation of thermal, mechanical and gas
796 barrier properties of polypropylene-modified clay nanocomposites by micro-
797 compounding process. *J. Taiwan Inst. Chem. Eng.* 88, 252–260.
798 <https://doi.org/https://doi.org/10.1016/j.jtice.2018.04.016>

799 Cao, M., Du, C., Guo, H., Songa, S., Li, X., Li, B., 2019. Continuous network of CNTs in
800 poly(vinylidene fluoride) composites with high thermal and mechanical performance for
801 heat exchangers. *Compos. Sci. Technol.* 173, 33–40.
802 <https://doi.org/10.1016/j.compscitech.2019.01.023>

803 Chatterjee, S., Nafezarefi, F., Tai, N.H., Schlagenhaut, L., Nüesch, F.A., Chu, B.T.T., 2012.
804 Size and synergy effects of nanofiller hybrids including graphene nanoplatelets and
805 carbon nanotubes in mechanical properties of epoxy composites. *Carbon N. Y.* 50,
806 5380–5386. <https://doi.org/10.1016/j.carbon.2012.07.021>

807 Chen, H., Ginzburg, V. V, Yang, J., Yang, Y., Liu, W., Huang, Y., Du, L., Chen, B., 2016.
808 Thermal conductivity of polymer-based composites: Fundamentals and applications.
809 *Prog. Polym. Sci.* 59, 41–85. <https://doi.org/10.1016/j.progpolymsci.2016.03.001>

810 Chiu, F., 2017a. Halloysite nanotube- and organoclay-filled biodegradable poly(butylene
811 succinate-co-adipate)/maleated polyethylene blend- based nanocomposites with
812 enhanced rigidity. *Compos. Part B* 110, 193–203.

813 Chiu, F., 2017b. Poly(vinylidene fluoride)/polycarbonate blend-based nanocomposites with
814 enhanced rigidity - Selective localization of carbon nanofillers and organoclay. *Polym.*

815 Test. 62, 115–123.
816 <https://doi.org/http://dx.doi.org/10.1016/j.polymeresting.2017.06.018>

817 Chiu, F.C., 2016. Fabrication and characterization of biodegradable poly(butylene succinate-
818 co-adipate) nanocomposites with halloysite nanotube and organo-montmorillonite as
819 nanofillers. *Polym. Test.* 54, 1–11. <https://doi.org/10.1016/j.polymeresting.2016.06.018>

820 Chiu, F.C., 2014. Comparisons of phase morphology and physical properties of PVDF
821 nanocomposites filled with organoclay and/or multi-walled carbon nanotubes. *Mater.*
822 *Chem. Phys.* 143, 681–692. <https://doi.org/10.1016/j.matchemphys.2013.09.054>

823 Cicco, D.D., Asaee, Z., Taheri, F., 2017. Use of nanoparticles for enhancing the interlaminar
824 properties of fibre-reinforced composites and adhesively bonded joints-a review.
825 *Nanomaterials* 7, 360. <https://doi.org/10.3390/nano7110360>

826 Das, S., Samal, S.K., Mohanty, S., Nayak, S.K., 2018. Crystallization of polymer blend
827 nanocomposites, in: Thomas, K.S., Mohammed, A.P., Gowd, E.B., Kalarikkal, N.
828 (Eds.), *Crystallization in Multiphase Polymer Systems*. Elsevier Inc., pp. 313–339.
829 <https://doi.org/10.1016/B978-0-12-809453-2.00011-6>

830 Dasari, A., Yu, Z.Z., Cai, G.P., Mai, Y.W., 2013. Recent developments in the fire retardancy
831 of polymeric materials. *Prog. Polym. Sci.* 38, 1357–1387.
832 <https://doi.org/10.1016/j.progpolymsci.2013.06.006>

833 Dlamini, D.S., Li, J., Mamba, B.B., 2019. Critical review of montmorillonite/polymer mixed-
834 matrix filtration membranes: Possibilities and challenges. *Appl. Clay Sci.* 168, 21–30.
835 <https://doi.org/10.1016/j.clay.2018.10.016>

836 Edenharter, A., Feicht, P., Diar-Bakerly, B., Beyer, G., Breu, J., 2016. Superior flame
837 retardant by combining high aspect ratio layered double hydroxide and graphene oxide.
838 *Polymer (Guildf)*. 91, 41–49. <https://doi.org/10.1016/j.polymer.2016.03.020>

839 El Rhazi, M., Majid, S., Elbasri, M., Salih, F.E., Oularbi, L., Lafdi, K., 2018. Recent progress

840 in nanocomposites based on conducting polymer: application as electrochemical sensors.
841 Int. Nano Lett. 8, 79–99. <https://doi.org/10.1007/s40089-018-0238-2>

842 Enotiadis, A., Litina, K., Gournis, D., Rangou, S., Avgeropoulos, A., Xidas, P.,
843 Triantafyllidis, K., 2013. Nanocomposites of polystyrene-b-poly(isoprene)-b-
844 polystyrene triblock copolymer with clay-carbon nanotube hybrid nanoadditives. J.
845 Phys. Chem. B 117, 907–915. <https://doi.org/10.1021/jp309361b>

846 Fang, C., Zhang, J., Chen, X., Weng, G.J., 2019. A Monte Carlo model with equipotential
847 approximation and tunneling resistance for the electrical conductivity of carbon
848 nanotube polymer composites. Carbon N. Y. 146, 125–138.
849 <https://doi.org/10.1016/j.carbon.2019.01.098>

850 Fanga, F., Ran, S., Fang, Z., Song, P., Wang, H., 2019. Improved flame resistance and
851 thermo-mechanical properties of epoxy resin nanocomposites from functionalized
852 graphene oxide via self-assembly in water. Compos. Part B 165, 406–416.
853 <https://doi.org/https://doi.org/10.1016/j.compositesb.2019.01.086>

854 Feng, Y., He, C., Wen, Y., Ye, Y., Zhou, X., Xie, X., Mai, Y.-W., 2018. Superior flame
855 retardancy and smoke suppression of epoxy-based composites with phosphorus/nitrogen
856 co-doped graphene. J. Hazard. Mater. 346, 140–151.
857 <https://doi.org/10.1016/j.jhazmat.2017.12.019>

858 Geng, C., Wang, J., Zhang, Q., Fu, Q., 2012. New piezoelectric damping composites of
859 poly(vinylidene fluoride) blended with clay and multi-walled carbon nanotubes. Polym.
860 Int. 61, 934–938. <https://doi.org/10.1002/pi.4161>

861 Golgoon, A., Aliofkhazraei, M., Toorani, M., Moradi, M.H., Rouhaghdam, A.S., 2015.
862 Corrosion and Wear Properties of Nanoclay- polyester Nanocomposite Coatings
863 Fabricated by Electrostatic Method. Procedia Mater. Sci. 11, 536–541.
864 <https://doi.org/10.1016/j.mspro.2015.11.042>

865 Gorrasi, G., D'Ambrosio, S., Patimo, G., Pantani, R., 2014. Hybrid clay-carbon
866 nanotube/PET composites: Preparation, processing, and analysis of physical properties.
867 J. Appl. Polym. Sci. 131, 1–7. <https://doi.org/10.1002/app.40441>

868 Gorrasi, G., Milone, C., Piperopoulos, E., Lanza, M., Sorrentino, A., 2013. Hybrid clay
869 mineral-carbon nanotube-PLA nanocomposite films. Preparation and photodegradation
870 effect on their mechanical, thermal and electrical properties. Appl. Clay Sci. 71, 49–54.
871 <https://doi.org/10.1016/j.clay.2012.11.004>

872 Gorrasi, G., Sorrentino, A., 2015. Mechanical milling as a technology to produce structural
873 and functional bio-nanocomposites. Green Chem. 17, 2610-2625.
874 <https://doi.org/10.1039/c5gc00029g>

875 Han, X., Zeng, X., Wang, J., Kong, D., Foster, N.R., Chen, J., 2016. Transparent flexible
876 ZnO/MWCNTs/pbma ternary nanocomposite film with enhanced mechanical properties.
877 Sci. China Chem. 59, 1010–1017. <https://doi.org/10.1007/s11426-015-0467-4>

878 Hapuarachchi, T.D., Peijs, T., 2010. Multiwalled carbon nanotubes and sepiolite nanoclays as
879 flame retardants for polylactide and its natural fibre reinforced composites. Compos.
880 Part A Appl. Sci. Manuf. 41, 954–963.
881 <https://doi.org/10.1016/j.compositesa.2010.03.004>

882 Hosseini, S.M., Yousefi, A.A., 2017a. Piezoelectric sensor based on electrospun PVDF-
883 MWCNT-Cloisite 30B hybrid nanocomposites. Org. Electron. 50, 121–129.
884 <https://doi.org/10.1016/j.orgel.2017.07.035>

885 Hosseini, S.M., Yousefi, A.A., 2017b. Electrospun PVDF/MWCNT/OMMT hybrid
886 nanocomposites: preparation and characterization. Iran. Polym. J. 26, 331–339.
887 <https://doi.org/10.1007/s13726-017-0522-4>

888 Isitman, N.A., Kaynak, C., 2010. Nanoclay and carbon nanotubes as potential synergists of
889 an organophosphorus flame-retardant in poly(methyl methacrylate). Polym. Degrad.

890 Stab. 95, 1523–1532. <https://doi.org/10.1016/j.polymdegradstab.2010.06.013>

891 Jaafar, M., 2017. Development of Hybrid Fillers/Polymer Nanocomposites for Electronic
892 Applications, in: Srivastava, S.K., Mittal, V. (Eds.), Hybrid Nanomaterials: Advances in
893 Energy, Environment and Polymer Nanocomposites. Scrivener , Wiley, pp. 349–369.
894 <https://doi.org/10.1002/9781119160380.ch7>

895 Ji, X., Chen, D., Wang, Q., Shen, J., Guo, S., 2018. Synergistic effect of flame retardants and
896 carbon nanotubes on flame retarding and electromagnetic shielding properties of
897 thermoplastic polyurethane. *Compos. Sci. Technol.* 163, 49–55.
898 <https://doi.org/https://doi.org/10.1016/j.compscitech.2018.05.007>

899 Kausar, A., 2016. Novel Polyamide Nanocomposite with Montmorillonite Clay and Gold
900 Nanoparticle Nanofillers. *Nanosci. Nanotechnol.* 6, 43–47.
901 <https://doi.org/10.5923/j.nn.20160603.02>

902 Kausar, A., Rafique, I., Muhammad, B., 2017. Aerospace Application of Polymer
903 Nanocomposite with Carbon nanotube, Graphite, Graphene Oxide and Nanoclay.
904 *Polym. Plast. Technol. Eng.* 56, 1438–1456.
905 <https://doi.org/https://doi.org/10.1080/03602559.2016.1276594>

906 Khajehpour, M., Arjmand, M., Sundararaj, U., 2014. Dielectric properties of multiwalled
907 carbon nanotube/ clay/polyvinylidene fluoride nanocomposites: effect of clay
908 incorporation. *Polym. Compos.* 37, 161–167. <https://doi.org/10.1002/pc.23167>

909 Khan, S., Bedi, H.S., Agnihotri, P.K., 2018. Augmenting mode-II fracture toughness of
910 carbon fibre/epoxy composites through carbon nanotube grafting. *Eng. Fract. Mech.*
911 204, 211–220. <https://doi.org/10.1016/j.engfracmech.2018.10.014>

912 Kim, H.S., Jang, J.U., Yu, J., Kim, S.Y., 2015. Thermal conductivity of polymer composites
913 based on the length of multi-walled carbon nanotubes. *Compos. Part B Eng.* 79, 505–
914 512. <https://doi.org/10.1016/j.compositesb.2015.05.012>

915 Klonos, P., Pissis, P., 2017. Effects of interfacial interactions and of crystallization on rigid
916 amorphous fraction and molecular dynamics in polylactide/silica nanocomposites: A
917 methodological approach. *Polymer (Guildf)*. 112, 228–243.
918 <https://doi.org/10.1016/j.polymer.2017.02.003>

919 Kumar, A., Kumar, K., Ghosh, P.K., Yadav, K.L., 2018. MWCNT/TiO₂ hybrid nano filler
920 toward high-performance epoxy composite. *Ultrason. Sonochem.* 41, 37–46.
921 <https://doi.org/10.1016/j.ultsonch.2017.09.005>

922 Kumar, S., Sun, L.L., Caceres, S., Li, B., Wood, W., Perugini, A., Maguire, R.G., Zhong,
923 W.H., 2010. Dynamic synergy of graphitic nanoplatelets and multi-walled carbon
924 nanotubes in polyetherimide nanocomposites. *Nanotechnology* 21, 105702.
925 <https://doi.org/10.1088/0957-4484/21/10/105702>

926 Kurahatti, R. V., Surendranathan, A.O., Kori, S.A., Singh, N., Kumar, A.V.R., Srivastava, S.,
927 2010. Defence applications of polymer nanocomposites. *Def. Sci. J.* 60, 551–563.
928 <https://doi.org/10.14429/dsj.60.578>

929 Lee, S., Kim, H. min, Seong, D.G., Lee, D., 2019. Synergistic improvement of flame
930 retardant properties of expandable graphite and multi-walled carbon nanotube reinforced
931 intumescent polyketone nanocomposites. *Carbon N. Y.* 143, 650–659.
932 <https://doi.org/10.1016/j.carbon.2018.11.050>

933 Levchenko, V., Mamunya, Y., Boiteux, G., Lebovka, M., Alcouffe, P., Seytre, G., Lebedev,
934 E., 2011. Influence of organo-clay on electrical and mechanical properties of
935 PP/MWCNT/OC nanocomposites. *Eur. Polym. J.* 47, 1351–1360.
936 <https://doi.org/10.1016/j.eurpolymj.2011.03.012>

937 Li, Y., Zhang, H., Liu, Y., Wang, H., Huang, Z., Peijs, T., Bilotti, E., 2018. Synergistic
938 effects of spray-coated hybrid carbon nanoparticles for enhanced electrical and thermal
939 surface conductivity of CFRP laminates. *Compos. Part A* 105, 9–18.

940 <https://doi.org/https://doi.org/10.1016/j.compositesa.2017.10.032>

941 Liu, L., Grunlan, J.C., 2007. Clay assisted dispersion of carbon nanotubes in conductive
942 epoxy nanocomposites. *Adv. Funct. Mater.* 17, 2343–2348.
943 <https://doi.org/10.1002/adfm.200600785>

944 Liu, W., Chen, Z., Cheng, X., Wang, Y., Amankwa, A.R., Xu, J., 2016. Design and ballistic
945 penetration of the ceramic composite armor. *Compos. Part B Eng.* 84, 33–40.
946 <https://doi.org/10.1016/j.compositesb.2015.08.071>

947 Liu, X., Guo, J., Tang, W., Li, H., Gu, X., Sun, J., Zhang, S., 2019. Enhancing the flame
948 retardancy of thermoplastic polyurethane by introducing montmorillonite nanosheets
949 modified with phosphorylated chitosan. *Compos. Part A* 119, 291–298.
950 <https://doi.org/https://doi.org/10.1016/j.compositesa.2019.02.009>

951 López-Barroso, J., Martínez-Hernández, A.L., Rivera-Armenta, J.L., Velasco-Santos, C.,
952 2018. Multidimensional nanocomposites of epoxy reinforced with 1D and 2D carbon
953 nanostructures for improve fracture resistance. *Polymers* 10, 281.
954 <https://doi.org/10.3390/polym10030281>

955 Ma, H., Tong, L., Xu, Z., Fang, Z., 2007. Synergistic effect of carbon nanotube and clay for
956 improving the flame retardancy of ABS resin. *Nanotechnology* 18, 375602.
957 <https://doi.org/10.1088/0957-4484/18/37/375602>

958 Madaleno, L., Pyrz, R., Crosky, A., Jensen, L.R., Rauhe, J.C.M., Dolomanova, V., Timmons,
959 A.M.M.V. de B., Pinto, J.J.C., Norman, J., 2013. Processing and characterization of
960 polyurethane nanocomposite foam reinforced with montmorillonite-carbon nanotube
961 hybrids. *Compos. Part A Appl. Sci. Manuf.* 44, 1–7.
962 <https://doi.org/10.1016/j.compositesa.2012.08.015>

963 Madaleno, L., Pyrz, R., Jensen, L.R., Pinto, J.J.C., Lopes, A.B., Dolomanova, V., Schjødt-
964 Thomsen, J., Rauhe, J.C.M., 2012. Synthesis of clay-carbon nanotube hybrids: Growth

965 of carbon nanotubes in different types of iron modified montmorillonite. *Compos. Sci.*
966 *Technol.* 72, 377–381. <https://doi.org/10.1016/j.compscitech.2011.11.027>

967 Manikandan, D., Mangalaraja, R.V., Avila, R.E., Siddheswaran, R., Ananthakumar, S., 2012.
968 Carbon nanotubes rooted montmorillonite (CNT-MM) reinforced nanocomposite
969 membrane for PEM fuel cells. *Mater. Sci. Eng. B Solid-State Mater. Adv. Technol.* 177,
970 614–618. <https://doi.org/10.1016/j.mseb.2012.02.027>

971 Manikandan, D., Viswanathan, R., Avila, R.E., Siddheswaran, R., Ananthakumar, S., 2013.
972 Montmorillonite – carbon nanotube nanofillers by acetylene decomposition using
973 catalytic CVD. *Appl. Clay Sci.* 71, 37–41. <https://doi.org/10.1016/j.clay.2012.10.001>

974 Marquis, D.M., Guillaume, E., Chivas-Joly, C., 2011. Properties of nanofillers in polymer,
975 Nanocomposites and polymers with analytical methods, in: Cuppoletti, J. (Ed.), .
976 *InTech*, Croatia. <https://doi.org/10.5772/21694>

977 Mayeen, A., Shaji, L.K., Nair, A.K., Kalarikkal, N., 2018. Morphological Characterization of
978 Nanomaterials, in: Bhagyaraj, S.M., Oluwafemi, O.S., Kalarikkal, N., Thomas, S. (Eds.),
979 *Characterization of Nanomaterials*. Elsevier Ltd., pp. 335–364.
980 <https://doi.org/10.1016/B978-0-08-101973-3.00012-2>

981 McCrum, N.G., Buckley, C.P., Bucknall, C.B., 1988. Principles of polymer engineering,
982 *Journal of Non-Newtonian Fluid Mechanics*. Oxford University Press, New York.
983 [https://doi.org/10.1016/0377-0257\(91\)80013-A](https://doi.org/10.1016/0377-0257(91)80013-A)

984 Moghri, M., Shamaee, H., Shahrajabian, H., Ghannadzadeh, A., 2015. The effect of different
985 parameters on mechanical properties of PA-6/clay nanocomposite through genetic
986 algorithm and response surface methods. *Int. Nano Lett.* 5, 133–140.
987 <https://doi.org/10.1007/s40089-015-0146-7>

988 Mohammed, N.A., 2014. Rheology, Processing and Properties of Polymer Nanocomposites
989 Based on POSS and Boehmite. PhD Thesis: Technische Universität, Berlin.

990 <https://doi.org/http://dx.doi.org/10.14279/depositonce-3981>

991 Navidfar, A., Sancak, A., Yildirim, K.B., Trabzon, L., 2017. A Study on Polyurethane Hybrid
992 Nanocomposite Foams Reinforced with Multiwalled Carbon Nanotubes and Silica
993 Nanoparticles. *Polym. - Plast. Technol. Eng.* 57, 1463–1473.
994 <https://doi.org/10.1080/03602559.2017.1410834>

995 Nayak, S., 2019. Dielectric Properties of Polymer -Carbon Composites, in: Rahaman, M.,
996 Khastgir, D., Aldalbahi, A.K. (Eds.), *Carbon-Containing Polymer Composites*. Springer
997 Series on Polymer and Composite Materials, Springer, Singapore, pp. 211–234.
998 https://doi.org/https://doi.org/10.1007/978-981-13-2688-2_6

999 Nurul, M.S., Mariatti, M., 2013. Effect of hybrid nanofillers on the thermal, mechanical, and
1000 physical properties of polypropylene composites. *Polym. Bull.* 70, 871–884.
1001 <https://doi.org/10.1007/s00289-012-0893-9>

1002 Olalekan, S.T., Muyibi, S.A., Shah, Q.H., Alkhatib, F.M., Yusof, F., Qudsieh, I.Y., 2010.
1003 Improving the Polypropylene-Clay Composite Using Carbon Nanotubes as Secondary
1004 Filler. *Energy Res. J.* 1, 68–72.

1005 Oliveira, A.D., Beatrice, C.A.G., Passador, F.R., Pessan, L.A., 2016. Polyetherimide-based
1006 nanocomposites materials for hydrogen storage. *AIP Conf. Proc.* 1779, 040006.
1007 <https://doi.org/10.1063/1.4965497>

1008 Pan, H., Pan, Y., Wang, W., Song, L., Hu, Y., Liew, K.M., 2014. Synergistic effect of layer-
1009 by-layer assembled thin films based on clay and carbon nanotubes to reduce the
1010 flammability of flexible polyurethane foam. *Ind. Eng. Chem. Res.* 53, 14315–14321.
1011 <https://doi.org/10.1021/ie502215p>

1012 Pandey, P., Mohanty, S., Nayak, S.K., 2014. Improved flame retardancy and thermal stability
1013 of polymer/clay nanocomposites, with the incorporation of multiwalled carbon nanotube
1014 as secondary filler: Evaluation of hybrid effect of nanofillers. *High Perform. Polym.* 26,

1015 826–836. <https://doi.org/10.1177/0954008314531802>

1016 Papageorgiou, D.G., Kinloch, I.A., Young, R.J., 2017a. Mechanical properties of graphene
1017 and graphene-based nanocomposites. *Prog. Mater. Sci.* 90, 75–127.
1018 <https://doi.org/10.1016/j.pmatsci.2017.07.004>

1019 Papageorgiou, D.G., Kinloch, I.A., Young, R.J., 2017b. Mechanical properties of graphene
1020 and graphene-based nanocomposites. *Prog. Mater. Sci.* 90, 75–127.
1021 <https://doi.org/http://dx.doi.org/10.1016/j.pmatsci.2017.07.004>

1022 Paszkiewicz, S., Szymczyk, A., Sui, X.M., Wagner, H.D., Linares, A., Cirera, A., Varea, A.,
1023 Ezquerro, T.A., Rosłaniec, Z., 2017. Electrical conductivity and transparency of polymer
1024 hybrid nanocomposites based on poly(trimethylene terephthalate) containing single
1025 walled carbon nanotubes and expanded graphite. *J. Appl. Polym. Sci.* 134, 44370.
1026 <https://doi.org/10.1002/app.44370>

1027 Peeterbroeck, S., Alexandre, M., Nagy, J.B., Pirlot, C., Fonseca, A., Moreau, N., Philippin,
1028 G., Delhalle, J., Mekhalif, Z., Sporken, R., Beyer, G., Dubois, P., 2004. Polymer-layered
1029 silicate-carbon nanotube nanocomposites: Unique nanofiller synergistic effect. *Compos.*
1030 *Sci. Technol.* 64, 2317–2323. <https://doi.org/10.1016/j.compscitech.2004.01.020>

1031 Pitchan, M.K., Bhowmik, S., Balachandran, M., Abraham, M., 2017. Process optimization of
1032 functionalized MWCNT/polyetherimide nanocomposites for aerospace application.
1033 *Mater. Des.* 127, 193–203. <https://doi.org/10.1016/j.matdes.2017.04.081>

1034 Pötschke, P., Kretschmar, B., Janke, A., 2007. Use of carbon nanotube filled polycarbonate
1035 in blends with montmorillonite filled polypropylene. *Compos. Sci. Technol.* 67, 855–
1036 860. <https://doi.org/10.1016/j.compscitech.2006.02.034>

1037 Potts, J.R., Lee, S.H., Alam, T.M., An, J., Stoller, M.D., Piner, R.D., Ruoff, R.S., 2011.
1038 Thermomechanical properties of chemically modified graphene/poly(methyl
1039 methacrylate) composites made by in situ polymerization. *Carbon N. Y.* 49, 2615–2623.

- 1040 <https://doi.org/10.1016/j.carbon.2011.02.023>
- 1041 Prasad, K.E., Das, B., Maitra, U., Ramamurty, U., Rao, C.N.R., 2009. Extraordinary synergy
1042 in the mechanical properties of polymer matrix composites reinforced with 2
1043 nanocarbons. *Proc. Natl. Acad. Sci.* 106, 13186–13189.
1044 <https://doi.org/10.1073/pnas.0905844106>
- 1045 Prashantha, K., Soulestin, J., Lacrampe, M.F., Krawczak, P., 2014. Processing and
1046 Characterization of Polypropylene Filled with Multiwalled Carbon Nanotube and Clay
1047 Hybrid Nanocomposites. *Int. J. Polym. Anal. Charact.* 19, 363–371.
1048 <https://doi.org/10.1080/1023666X.2014.902715>
- 1049 Punetha, V.D., Rana, S., Yoo, H.J., Chaurasia, A., McLeskey, J.T., Ramasamy, M.S., Sahoo,
1050 N.G., Cho, J.W., 2017. Functionalization of carbon nanomaterials for advanced polymer
1051 nanocomposites: A comparison study between CNT and graphene. *Prog. Polym. Sci.* 67,
1052 1–47. <https://doi.org/10.1016/j.progpolymsci.2016.12.010>
- 1053 Radmanesh, F., Rijnaarts, T., Moheb, A., Sadeghi, M., de Vos, W.M., 2019. Enhanced
1054 selectivity and performance of heterogeneous cation exchange membranes through
1055 addition of sulfonated and protonated Montmorillonite. *J. Colloid Interface Sci.* 533,
1056 658–670. <https://doi.org/10.1016/j.jcis.2018.08.100>
- 1057 Raee, E., Kaffashi, B., 2018. Biodegradable polypropylene/thermoplastic starch
1058 nanocomposites incorporating halloysite nanotubes. *J. Appl. Polym. Sci.* 135, 45740.
1059 <https://doi.org/10.1002/app.45740>
- 1060 Rahmaoui, F.E.Z., Mederic, P., Aït Hocine, N., Aït Saada, A., Poirot, N., Belaidi, I., 2017.
1061 Applied Clay Science Contribution of the organo-montmorillonite / graphene pair to the
1062 rheological and mechanical properties of polyethylene matrix based nanocomposites.
1063 *Appl. Clay Sci.* 150, 244–251. <https://doi.org/10.1016/j.clay.2017.09.037>
- 1064 Raji, M., Mekhzoum, M.E.M., Qaiss, A.K., Bouhfid, R., 2016. Nanoclay Modification and

1065 Functionalization for Nanocomposites Development: Effect on the Structural,
1066 Morphological, Mechanical and Rheological Properties, in: Jawaid, M., Qaiss, A.,
1067 Bouhfid, R. (Eds.), Nanoclay Reinforced Polymer Composites, Engineering Materials.
1068 Springer, Singapore, pp. 1–34. <https://doi.org/10.1007/978-981-10-1953-1>

1069 Raji, M., Mekhzouma, M.M., Rodrigue, D., Qaissa, A., Bouhfi, R., 2018. Effect of silane
1070 functionalization on properties of polypropylene/clay nanocomposites. *Compos. Part B*
1071 146, 106–115. <https://doi.org/10.1016/j.compositesb.2018.04.013>

1072 Ramazanov, M.A., Maharramov, A.M., Ali-zada, R.A., Shirinova, H.A., Hajiyeva, F. V.,
1073 2018. Theoretical and experimental investigation of the magnetic properties of
1074 polyvinylidene fluoride and magnetite nanoparticles-based nanocomposites. *J. Theor.*
1075 *Appl. Phys.* 12, 7–13. <https://doi.org/10.1007/s40094-018-0282-3>

1076 Rao, B.N., Praveen, T.A., Sailaja, R.R.N., Khan, M.A., 2015. HDPE Nanocomposites Using
1077 Nanoclay, MWCNT and Intumescent Flame Retardant Characteristics, in: 2015 IEEE
1078 11th International Conference on the Properties and Applications of Dielectric Materials
1079 (ICPADM). pp. 812–815. <https://doi.org/10.1109/icpadm.2015.7295396>

1080 Ray, S.S., Okamoto, M., 2003. Polymer/layered silicate nanocomposites: A review from
1081 preparation to processing. *Prog. Polym. Sci.* 28, 1539–1641.
1082 <https://doi.org/10.1016/j.progpolymsci.2003.08.002>

1083 Ren, J., Dang, K.M., Pollet, E., Avérous, L., 2018. Preparation and characterization of
1084 thermoplastic potato starch/halloysite nano-biocomposites: Effect of plasticizer nature
1085 and nanoclay content. *Polymers (Basel)*. 10. <https://doi.org/10.3390/polym10080808>

1086 Roes, A.L., Marsili, E., Nieuwlaar, E., Patel, M.K., 2007. Environmental and cost assessment
1087 of a polypropylene nanocomposite. *J. Polym. Environ.* 15, 212–226.
1088 <https://doi.org/10.1007/s10924-007-0064-5>

1089 Rotheron, R.N., Hornsby, P.R., 1996. Flame retardant effects of magnesium hydroxide. *Polym.*

1090 Degrad. Stab. 54, 383–385. [https://doi.org/10.1016/S0141-3910\(96\)00067-5](https://doi.org/10.1016/S0141-3910(96)00067-5)

1091 Rueda, M.M., Auscher, M.C., Fulchiron, R., Périé, T., Martin, G., Sonntag, P., Cassagnau, P.,
1092 2017. Rheology and applications of highly filled polymers: A review of current
1093 understanding. Prog. Polym. Sci. 66, 22–53.
1094 <https://doi.org/10.1016/j.progpolymsci.2016.12.007>

1095 Sa, K., Mahakul, P.C., Subramanyam, B.V.R.S., Raiguru, J., Das, S., Alam, I., Mahanandia,
1096 P., 2018. Effect of reduced graphene oxide-carbon nanotubes hybrid nanofillers in
1097 mechanical properties of polymer nanocomposites. IOP Conf. Ser. Mater. Sci. Eng. 338,
1098 012055. <https://doi.org/10.1088/1757-899X/338/1/012055>

1099 Safdari, M., Al-haik, M.S., 2018. A Review on Polymeric Nanocomposites: Effect of
1100 Hybridization and Synergy on Electrical Properties, in: Ismail, A.F., Goh, P.S. (Eds.),
1101 Carbon-Based Polymer Nanocomposites for Environmental and Energy Applications.
1102 Elsevier, Amsterdam, pp. 113–146. [https://doi.org/10.1016/B978-0-12-813574-7.00005-](https://doi.org/10.1016/B978-0-12-813574-7.00005-8)
1103 8

1104 Safdari, M., Al-Haik, M.S., 2013. Synergistic electrical and thermal transport properties of
1105 hybrid polymeric nanocomposites based on carbon nanotubes and graphite
1106 nanoplatelets. Carbon N. Y. 64, 111–121. <https://doi.org/10.1016/j.carbon.2013.07.042>

1107 Santangelo, S., Gorrasi, G., Di Lieto, R., De Pasquale, S., Patimo, G., Piperopoulos, E.,
1108 Lanza, M., Faggio, G., Mauriello, F., Messina, G., Milone, C., 2011. Polylactide and
1109 carbon nanotubes/smectite-clay nanocomposites: Preparation, characterization, sorptive
1110 and electrical properties. Appl. Clay Sci. 53, 188–194.
1111 <https://doi.org/10.1016/j.clay.2010.12.013>

1112 Seghar, S., Azem, S., Aït Hocine, N., 2011. Effects of clay nanoparticles on the mechanical
1113 and physical properties of unsaturated polyester. Adv. Sci. Lett. 4, 3424–3430.
1114 <https://doi.org/10.1166/asl.2011.2051>

- 1115 Shabanian, M., Hajibeygi, M., Hedayati, K., Khaleghi, M., Khonakdar, H.A., 2016. New
1116 ternary PLA/organoclay-hydrogel nanocomposites: Design, preparation and study on
1117 thermal, combustion and mechanical properties. *Mater. Des.* 110, 811–820.
1118 <https://doi.org/10.1016/j.matdes.2016.08.059>
- 1119 Shao, L., Shi, L., Li, X., Song, N., Ding, P., 2016. Synergistic effect of BN and graphene
1120 nanosheets in 3D framework on the enhancement of thermal conductive properties of
1121 polymeric composites. *Compos. Sci. Technol.* 135, 83–91.
1122 <https://doi.org/10.1016/j.compscitech.2016.09.013>
- 1123 Shirvanimoghaddam, K., Abolhasani, M.M., Li, Q., Khayyam, H., Naebe, M., 2017. Cheetah
1124 skin structure: A new approach for carbon-nano-patterning of carbon nanotubes.
1125 *Compos. Part A Appl. Sci. Manuf.* 95, 304–314.
1126 <https://doi.org/10.1016/j.compositesa.2017.01.023>
- 1127 Shirvanimoghaddam, K., Abolhasani, M.M., Poliseti, B., Naebe, M., 2018. Periodical
1128 patterning of a fully tailored nanocarbon on CNT for fabrication of thermoplastic
1129 composites. *Compos. Part A Appl. Sci. Manuf.* 107, 304–314.
1130 <https://doi.org/10.1016/j.compositesa.2018.01.015>
- 1131 Silva, B.L., Nack, F.C., Lepienski, C.M., Coelho, L.A.F., Becker, D., 2014. Influence of
1132 intercalation methods in properties of Clay and carbon nanotube and high density
1133 polyethylene nanocomposites. *Mater. Res.* 17, 1628–1636. <https://doi.org/10.1590/1516-1439.303714>
- 1135 Singla, R.K., Zafar, M.T., Maiti, S.N., Ghosh, A.K., 2017. Physical blends of PLA with high
1136 vinyl acetate containing EVA and their rheological, thermo-mechanical and
1137 morphological responses. *Polym. Test.* 63, 398–406.
1138 <https://doi.org/10.1016/j.polymertesting.2017.08.042>
- 1139 Stern, N., Dyamant, I., Shemer, E., Hu, X., Marom, G., 2018. Hybrid effects in the fracture

1140 toughness of polyvinyl butyral-based nanocomposites. *Nanocomposites* 4, 1–9.
1141 <https://doi.org/10.1080/20550324.2018.1447827>

1142 Surendran, A., Pionteck, J., Vogel, R., Kalarikkal, N., Geethamma, V.G., Thomas, S., 2018.
1143 Effect of organically modified clay on the morphology, rheology and viscoelasticity of
1144 epoxy-thermoplastic nanocomposites. *Polym. Test.* 70, 18–29.
1145 <https://doi.org/https://doi.org/10.1016/j.polymertesting.2018.06.023>

1146 Szeluga, U., Kumanek, B., Trzebicka, B., 2015. Synergy in hybrid polymer/nanocarbon
1147 composites. A review. *Compos. Part A Appl. Sci. Manuf.* 73, 204–231.
1148 <https://doi.org/10.1016/j.compositesa.2015.02.021>

1149 Terzopoulou, Z., Bikiaris, D.N., Triantafyllidis, K.S., Potsi, G., Gournis, D., Papageorgiou,
1150 G.Z., Rudolf, P., 2016. Mechanical, thermal and decomposition behaviour of poly(ϵ -
1151 caprolactone) nanocomposites with clay-supported carbon nanotube hybrids.
1152 *Thermochim. Acta* 642, 67–80. <https://doi.org/10.1016/j.tca.2016.09.001>

1153 Tjong, S.C., 2014. Synthesis and Structural-Mechanical Property Characteristics of
1154 Graphene-Polymer Nanocomposites, in: Tjong, S. C. (Ed.), *Nanocrystalline Materials:
1155 Their Synthesis-Structure-Property Relationships and Applications*. Elsevier,
1156 Amsterdam, pp. 335–375. <https://doi.org/10.1016/B978-0-12-407796-6.00010-5>

1157 Tsai, T.Y., Naveen, B., Shiu, W.C., Lu, S.W., 2014. An advanced preparation and
1158 characterization of the PET/MgAl-LDH nanocomposites. *RSC Adv.* 4, 25683–25691.
1159 <https://doi.org/10.1039/c4ra03171g>

1160 Usuki, A., Yoshitsugu, K., Masaya, K., Akane, O., Yoshiaki, F., Toshio, K., Osami, K., 1993.
1161 Synthesis of Nylon 6-clay hybrid. *J. Mater. Res.* 8, 1179–1184.
1162 <https://doi.org/10.1557/JMR.1993.1179>

1163 Venkategowda, C., Rajanna, S., Udupa, N.G.S., Keshavamurthy, R., 2018. Experimental
1164 investigation of glass- carbon/epoxy hybrid composites subjected to low velocity impact

1165 test. FME Trans. 46, 595–602. <https://doi.org/10.5937/fmet1804595R>

1166 Vyas, M.K., Chandra, A., 2018. Role of organic/inorganic salts and nanofillers in polymer
1167 nanocomposites: enhanced conduction, rheological, and thermal properties. J. Mater.
1168 Sci. 53, 4987–5003. <https://doi.org/10.1007/s10853-017-1912-x>

1169 Wang, J.Y., Yang, S.Y., Huang, Y.L., Tien, H.W., Chin, W.K., Ma, C.C.M., 2011.
1170 Preparation and properties of graphene oxide/polyimide composite films with low
1171 dielectric constant and ultrahigh strength via in situ polymerization. J. Mater. Chem. 21,
1172 13569–13575. <https://doi.org/10.1039/c1jm11766a>

1173 Wang, S., Gao, R., Zhou, K., 2019. The influence of cerium dioxide functionalized reduced
1174 graphene oxide on reducing fire hazards of thermoplastic polyurethane nanocomposites.
1175 J. Colloid Interface Sci. 536, 127–134.
1176 <https://doi.org/https://doi.org/10.1016/j.jcis.2018.10.052>

1177 Wani, T.P., Rajab, R., Sampathkumaran, P., Seetharamu, S., 2018. Investigation on Wear and
1178 Friction Characteristics of Bi-Directional Silk Fibre Reinforced Nanoclay Added HDPE
1179 Composites. Mater. Today Proc. 5, 25713–25719.
1180 <https://doi.org/https://doi.org/10.1016/j.matpr.2018.11.013>

1181 Wu, Z., Wang, H., Zheng, K., Xue, M., Cui, P., Tian, X., 2012. Incorporating strong polarity
1182 minerals of tourmaline with carbon nanotubes to improve the electrical and
1183 electromagnetic interference shielding properties. J. Phys. Chem. C 116, 12814–12818.
1184 <https://doi.org/10.1021/jp2121164>

1185 Xiao, Y., Wang, W. yan, Chen, X. jia, Lin, T., Zhang, Y. tong, Yang, J. hui, Wang, Y., Zhou,
1186 Z. wan, 2016. Hybrid network structure and thermal conductive properties in
1187 poly(vinylidene fluoride) composites based on carbon nanotubes and graphene
1188 nanoplatelets. Compos. Part A Appl. Sci. Manuf. 90, 614–625.
1189 <https://doi.org/10.1016/j.compositesa.2016.08.029>

1190 Xu, Z., Gao, C., 2010. In situ polymerization approach to graphene-reinforced nylon-6
1191 composites. *Macromolecules* 43, 6716–6723. <https://doi.org/10.1021/ma1009337>

1192 Yang, S.Y., Lin, W.N., Huang, Y.L., Tien, H.W., Wang, J.Y., Ma, C.C.M., Li, S.M., Wang,
1193 Y.S., 2011. Synergetic effects of graphene platelets and carbon nanotubes on the
1194 mechanical and thermal properties of epoxy composites. *Carbon N. Y.* 49, 793–803.
1195 <https://doi.org/10.1016/j.carbon.2010.10.014>

1196 Yuan, B., Fan, A., Yang, M., Chen, X., Hu, Y., Bao, C., Jiang, S., Niu, Y., Zhang, Y., He, S.,
1197 Dai, H., 2017. The effects of graphene on the flammability and fire behaviour of
1198 intumescent flame retardant polypropylene composites at different flame scenarios,
1199 *Polymer Degradation and Stability*. Elsevier Ltd.
1200 <https://doi.org/10.1016/j.polymdegradstab.2017.06.015>

1201 Yuan, B., Sun, Y., Chen, X., Shi, Y., Dai, H., He, S., 2018. Poorly-/well-dispersed graphene:
1202 Abnormal influence on flammability and fire behaviour of intumescent flame retardant.
1203 *Compos. Part A Appl. Sci. Manuf.* 109, 345–354.
1204 <https://doi.org/10.1016/j.compositesa.2018.03.022>

1205 Yue, L., Pircheraghi, G., Monemian, S.A., Manas-Zloczower, I., 2014. Epoxy composites
1206 with carbon nanotubes and graphene nanoplatelets - Dispersion and synergy effects.
1207 *Carbon N. Y.* 78, 268–278. <https://doi.org/10.1016/j.carbon.2014.07.003>

1208 Zaferani, S.H., 2018. Introduction of polymer-based nanocomposites, in: Jawaid, M., Khan,
1209 M. (Eds.), *Polymer-Based Nanocomposites for Energy and Environmental Applications*.
1210 Woodhead Publishing, Elsevier, pp. 1–25. [https://doi.org/10.1016/B978-0-08-102262-](https://doi.org/10.1016/B978-0-08-102262-7.00001-5)
1211 [7.00001-5](https://doi.org/10.1016/B978-0-08-102262-7.00001-5)

1212 Zhang, H., Zhang, G., Tang, M., Zhou, L., Li, J., Fan, X., Shi, X., Qin, J., 2018. Synergistic
1213 effect of carbon nanotube and graphene nanoplates on the mechanical, electrical and
1214 electromagnetic interference shielding properties of polymer composites and polymer

1215 composite foams. *Chem. Eng. J.* 353, 381–393. <https://doi.org/10.1016/j.cej.2018.07.144>

1216 Zhang, W.-D., Phang, I.Y., Liu, T., 2006. Growth of Carbon Nanotubes on Clay: Unique
1217 Nanostructured Filler for High-Performance Polymer Nanocomposites. *Adv. Mater.* 18,
1218 73–77. <https://doi.org/10.1002/adma.200501217>

1219 Zhao, B., Wang, S., Zhao, C., Li, R., Hamidinejad, S.M., Kazemi, Y., Park, C.B., 2018.
1220 Synergism between carbon materials and Ni chains in flexible poly(vinylidene fluoride)
1221 composite films with high heat dissipation to improve electromagnetic shielding
1222 properties. *Carbon N. Y.* 127, 469–478. <https://doi.org/10.1016/j.carbon.2017.11.032>

1223 Zhao, Y.-Q., Lau, K.-T., Wang, Z., Wang, Z.-C., Cheung, H.-Y., Yang, Z., Li, H.-L., 2009.
1224 Fabrication and Properties of Clay-Supported Carbon Nanotube/Poly (vinyl alcohol)
1225 Nanocomposites. *Polym. Compos.* 30, 702–707. <https://doi.org/10.1002/pc.20698>

1226 Zhou, E., Xi, J., Guo, Y., Liu, Y., Xu, Z., Peng, L., Gao, W., Ying, J., Chen, Z., Gao, C.,
1227 2018. Synergistic effect of graphene and carbon nanotube for high-performance
1228 electromagnetic interference shielding films. *Carbon N. Y.* 133, 316–322.
1229 <https://doi.org/10.1016/j.carbon.2018.03.023>

1230 Zhu, T., Qian, C., Zheng, W., Bei, R., Liu, S., Chi, Z., Chen, X., Zhang, Y., Xu, J., 2018.
1231 Modified halloysite nanotube filled polyimide composites for film capacitors: High
1232 dielectric constant, low dielectric loss and excellent heat resistance. *RSC Adv.* 8, 10522–
1233 10531. <https://doi.org/10.1039/c8ra01373j>

1234 Zhu, T.T., Zhou, C.H., Kabwe, F.B., Wu, Q.Q., Li, C.S., Zhang, J.R., 2019. Exfoliation of
1235 montmorillonite and related properties of clay/polymer nanocomposites. *Appl. Clay Sci.*
1236 169, 48–66. <https://doi.org/https://doi.org/10.1016/j.clay.2018.12.006>

Graphical abstract:

